Nilsen, K. T., B. C. Vendeville, J.-T. Johansen, 1995, Influence of regional tectonics on halokinesis in the Nordkapp Basin, Barents Sea, *in* M. P. A. Jackson, D. G. Roberts, and S. Snelson, eds., Salt tectonics: a global perspective: AAPG Memoir 65, p. 413–436.

Chapter 20

Influence of Regional Tectonics on Halokinesis in the Nordkapp Basin, Barents Sea

Kåre T. Nilsen
Norwegian Petroleum Directorate
Harstad, Norway

Bruno C. Vendeville
Bureau of Economic Geology
The University of Texas at Austin
Austin, Texas, U.S.A.

Jan-Terje Johansen
Norwegian Petroleum Directorate
Harstad, Norway

Abstract

Seismic analysis of salt structures in the Nordkapp Basin, a deep salt basin in the southern Barents Sea, combined with experimental modeling suggests that regional tectonics closely controlled diapiric growth. Diapirs formed in the Early Triassic during basement-involved regional extension. The diapirs then rose rapidly by passive growth and exhausted their source layer. Regional extension in the Middle–Late Triassic triggered down-to-the-basin gravity gliding, which laterally shortened the diapirs. This squeezed salt out of diapir stems, forcing diapirs to rise, extrude, and form diapir overhangs. After burial under more than 1000 m of Upper Triassic–Lower Cretaceous sediments, the diapirs were rejuvenated by a Late Cretaceous episode of regional extension and gravity gliding, which deformed their thick roofs. After extension, diapirs stopped rising and were buried under 1500 m of lower Tertiary sediments. Regional compression of the Barents Sea region in the middle Tertiary caused one more episode of diapiric rise. Diapirs in the Nordkapp Basin are now extinct.

INTRODUCTION

The Nordkapp Basin (Figure 1) is a deep, narrow salt basin in the southern Barents Sea. The southwestern part of the Nordkapp Basin is a narrow, northeast-trending subbasin 150 km long and 25–50 km wide; about 17 salt domes are located along the basin's axis (Figure 2a). The northeastern part (Figure 2a) is a wider, east-trending subbasin about 200 km long and 50–70 km wide. More than 16 salt domes occur west of the 32°E meridian (no exploration has been conducted east of here). Exploration in the Nordkapp Basin started in the 1980s but remained limited until the early 1990s. Only one well has been drilled so far, although another well is scheduled for 1996. Published work on the Nordkapp Basin (e.g., Gabrielsen et al., 1990) remained scarce until the 1992 Norwegian Petroleum Society (NPF) special publication *Structural and Tectonic Modelling and Its Applications to Petroleum Geology* (e.g., Dengo and Røssland, 1992; Gabrielsen et al., 1992; Jensen and Sørensen, 1992). Recently, the oil industry showed renewed interest in the basin during the 14th concession round in 1993 (Jensen et al., 1993). Furthermore, recent improvements in the interpretation of the basin's structural history and discovery of traces of hydrocarbons in wells outside the basin suggest that the Nordkapp Basin could soon become a promising exploration target.

As the quality of seismic data and structural interpretations has improved, the inferred geometry of salt structures in the basin has progressed from wide salt stocks with vertical flanks to more complex shapes with broad diapir overhangs above narrow stems (Koyi et al., 1993; Talbot et al., 1993; Yu and Lerche, 1993). These refined interpretations have reduced the estimates of the total volume of salt remaining in the basin (Koyi et al., 1993). Also, new seismic data with higher resolution have imaged numerous normal faults in the subsalt basement on the margins (Gabrielsen et al., 1992) and in the basin itself (Koyi et al., 1993).

Since 1993, the Norwegian Petroleum Directorate (Harstad, Norway) and the Applied Geodynamics Laboratory (Bureau of Economic Geology, The University

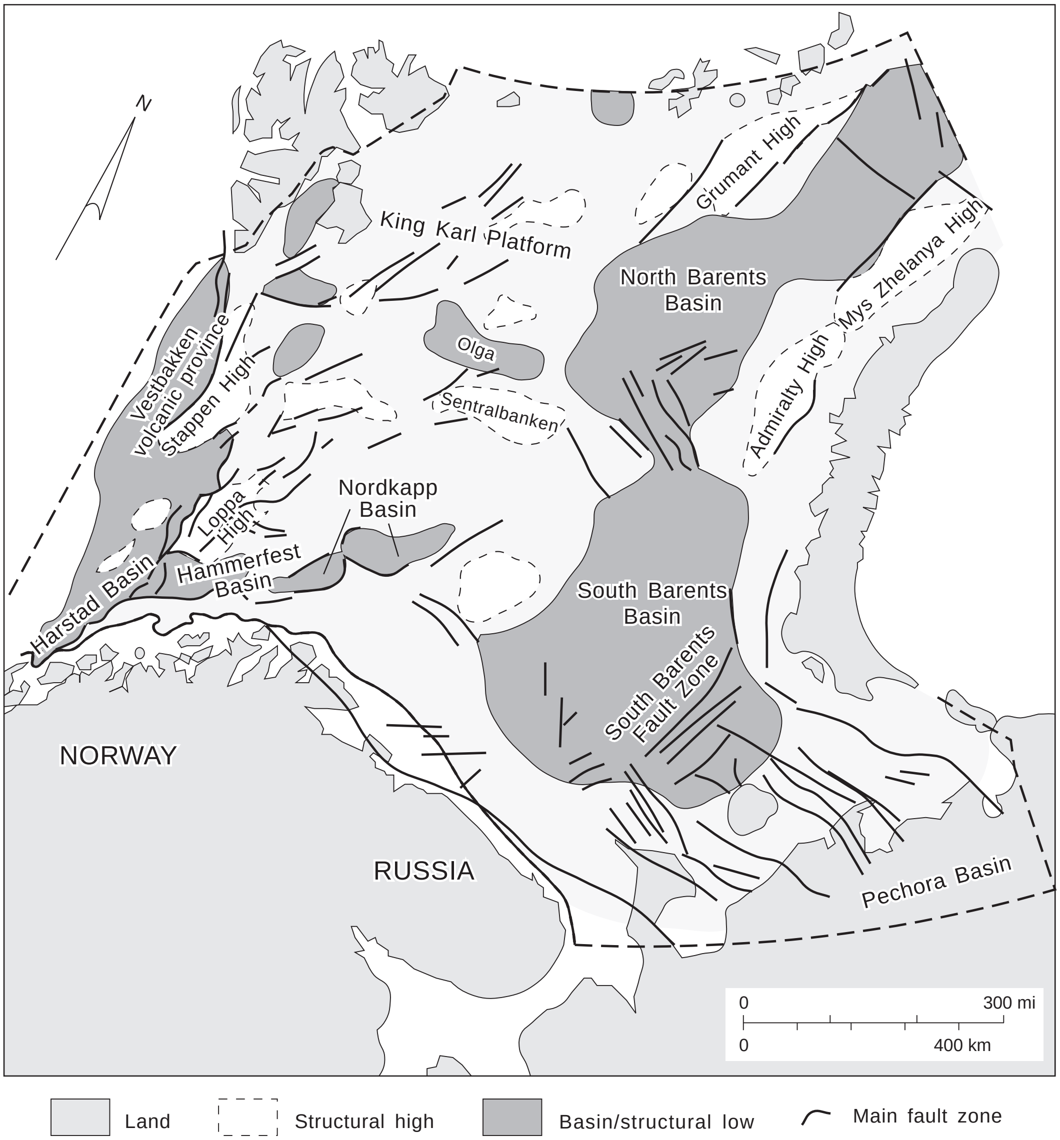

Figure 1—Main structural elements in the Barents Sea area and location of the Nordkapp Basin. Modified from Johansen et al. (1993).

of Texas at Austin) have conducted a detailed structural study of the Nordkapp Basin applying concepts derived from scaled tectonic experiments (e.g., Nilsen et al., 1994; Vendeville et al., 1994). This combination has helped to refine the structural interpretation of salt tectonics. In this chapter, we focus on how regional tectonics in the Barents Sea has tightly controlled the initiation, growth, and reactivation of salt structures in the Nordkapp Basin (Figure 3). Salt tectonics in the Nordkapp Basin is characterized by short periods of diapiric growth, commonly corresponding to regional tectonic phases, interspersed between longer intervals of diapiric inactivity during regional tectonic lulls. We show that successive phases of regional extension (1) formed the initial basin in which rock salt was deposited during the late Paleozoic, (2) initiated Early Triassic diapiric rise by fracturing the salt overburden, and (3) triggered gravity gliding during Middle–Late Triassic and Late Cretaceous time, thereby forcing the diapirs to rise after source layer depletion, even after they had been capped by thick sedimentary roofs. Middle Tertiary regional shortening also reactivated the diapirs.

LATE PALEOZOIC: FORMATION OF THE NORDKAPP BASIN

Seismic sections along the margins of the basin (Figure 4) (e.g., Gabrielsen et al., 1992) clearly show the offsets of subsalt strata across basement faults. In contrast, in the deeper, central part of the basin, subsalt faults are commonly obscured by seismic noise because of the overlying diapirs and folded or faulted suprasalt strata (Figure 5). Free-air gravity data help delineate the basin's

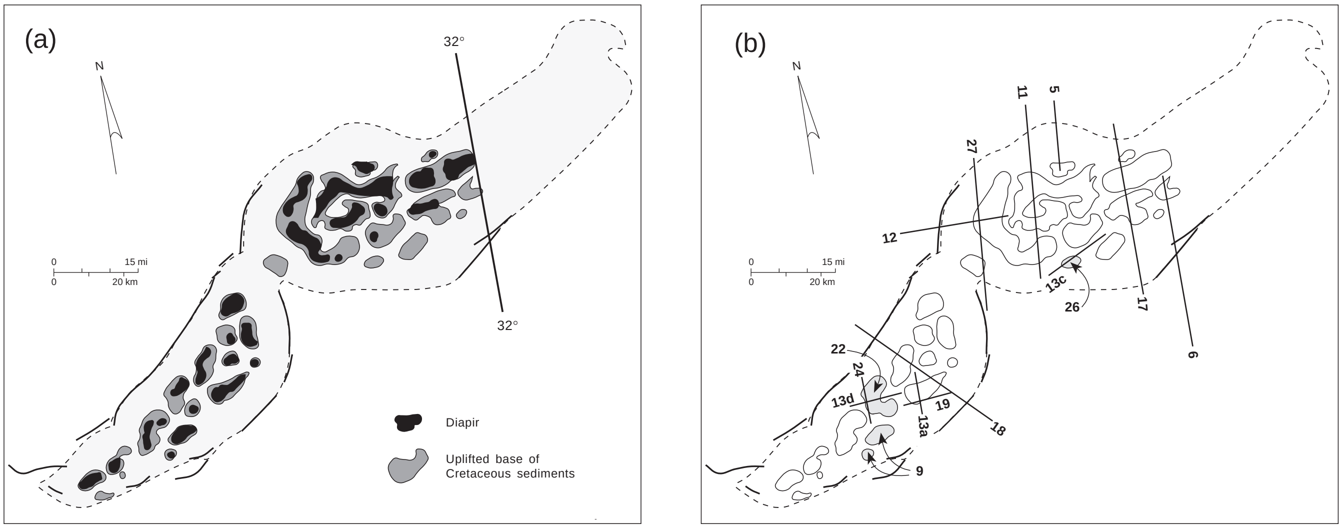

(above)

Figure 2—(a) Simplified structural map of the Nordkapp Basin showing salt diapirs and main fault zones. The map shows no diapirs east of longitude 32˚E because of the absence of exploration data here, not because of the lack of diapirs. Black = subcrop of diapirs at or near the Pliocene–Pleistocene erosion surface; dark stippled = base of Cretaceous sediments uplifted above regional datum during diapiric rise. (b) Location map for section lines and detail maps (stippled diapirs) in Figures 5–27. Numbers on the map correspond to figure numbers.

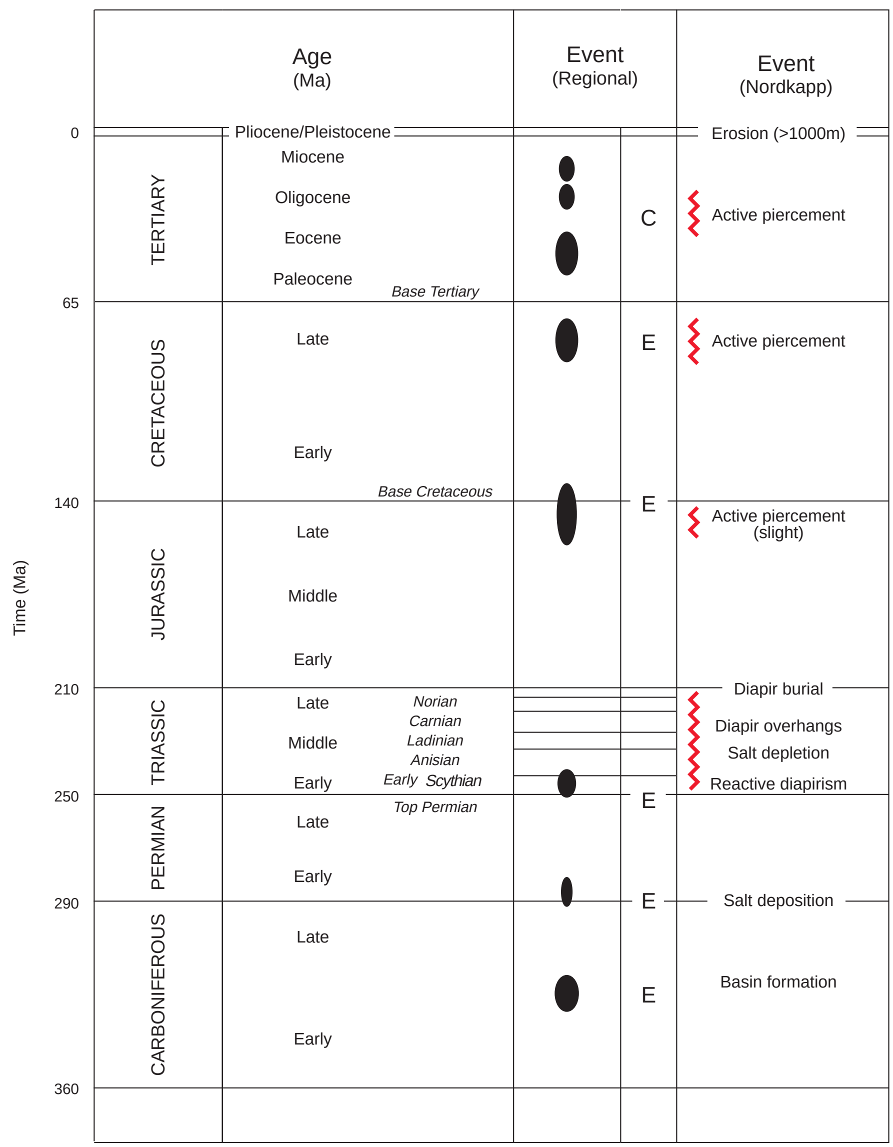

Figure 3—Time chart showing the connection between diapiric history in the Nordkapp Basin and regional tectonic events in the Barents Sea area. E and C denote episodes of regional extension and compression, respectively, illustrated by black ellipses.

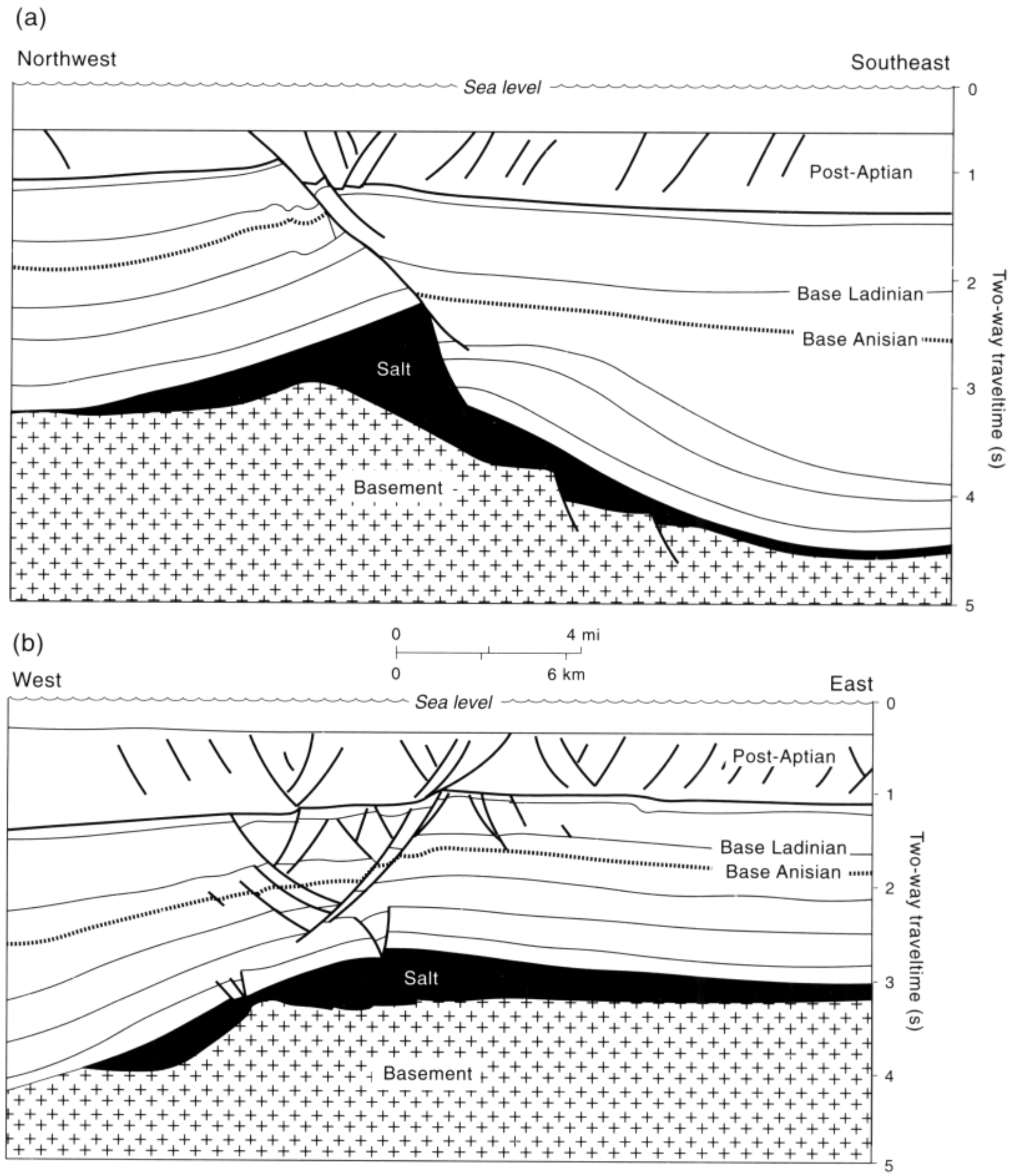

Figure 4—Salt rollers and normal faults on the margins of the southwestern Nordkapp Basin. Line tracings from (a) northwest-southeast and (b) west-east seismic sections by Gabrielsen et al. (1992). Sections also show faults in the subsalt basement; normal faults in the overburden remained active until Cretaceous time. Cross pattern = subsalt basement; black = salt; white = over-burden; dotted line = base of Anisian (Middle Triassic); thick line = base of Cretaceous.

geometry in the subsalt basement as a 25- to 70-km-wide, 350-km-long northeast-trending basin made of two segments separated by an intrabasin ridge (Dengo and Rørssland, 1992; Gudlaugson et al., 1994). The initial basement faulting is attributed to a phase of regional extension during the middle Carboniferous that created the basic architecture of grabens, half-grabens, and basement highs in the Barents Sea (Stemmerik and Worsley, 1989; Dengo and Rørssland, 1992; Gabrielsen et al., 1992; Jensen and Sørensen, 1992; Gudlaugson et al., 1994; Johansen et al., 1994). By correlation with regional tectonics on the Finnmark platform, the tectonic event responsible for the formation of the basin can be dated as Serphukopian (Early–middle Carboniferous). The structural grain inherited from the Caledonian orogeny probably partially controlled the deformation style of the presalt units (Kjøde et al., 1978; Dore, 1991; Karpaz et al., 1993; Gudlaugson et al., 1994; Lippard, 1994; Nilsen, 1994). Seismic sections across the Nordkapp Basin show asymmetric half-grabens and grabens whose polarity shifts rapidly along the basin's strike (Bergendahl, 1989; Gabrielsen et al., 1990, 1992; Dengo and Rørssland, 1992; Gudlaugson et al., 1994). In the southwestern Nordkapp Basin, the dominant fault vergence shifts from northwest-facing faults in the south (Måsøy fault complex) to southeast-facing faults in the north (Nordsel High along the Nysleppen fault complex). In the intrabasin high, basement faults and grabens are more symmetric. The northeastern subbasin shows similar shifts in dominant fault polarity along the basin strike.

After rifting, a thick, Upper Carboniferous–Lower Permian layer of evaporites was deposited in the basin and partially overstepped the basin margins (Gerard and Buhrig, 1990; Bruce and Toomy, 1993; Nilsen et al., 1993).

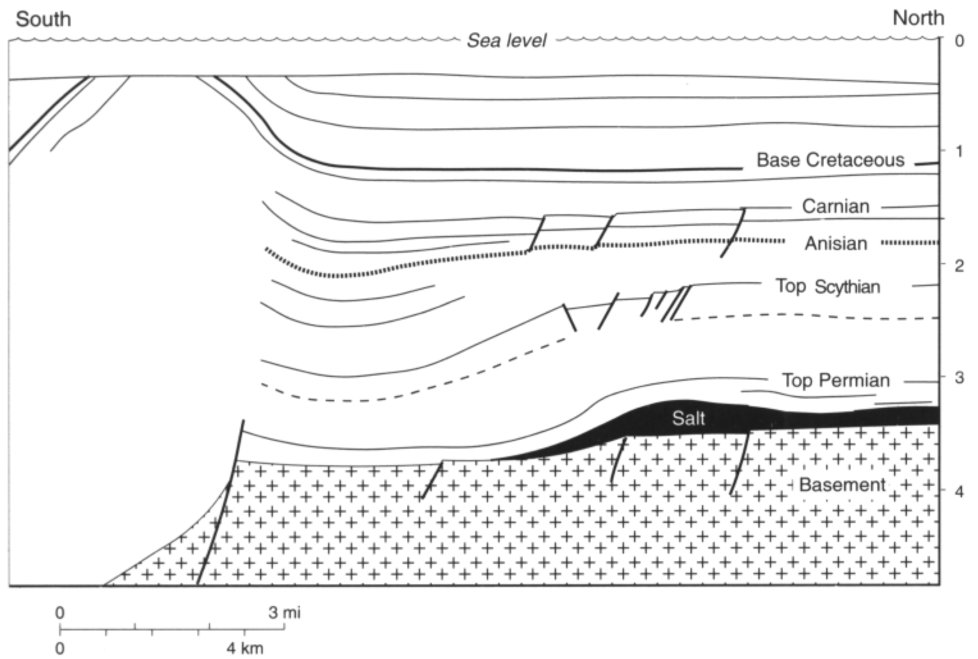

Figure 5—Line drawing from seismic section (Norwegian Petroleum Directorate line 302230-86) along the northern margin of the Nordkapp Basin. (See Figure 2b for location.) Section shows normal faults formed by Early Triassic regional extension (top of Scythian). Similar normal faults are suspected to have initiated diapirs in the basin but cannot be imaged in seismic reflection (e.g., left side of diapir). Also note basinward stratigraphic thickening of the Middle–Upper Triassic (top of Scythian–Anisian) associated with rapid passive diapiric growth. Black = salt; dotted line = base of Anisian (Middle Triassic).

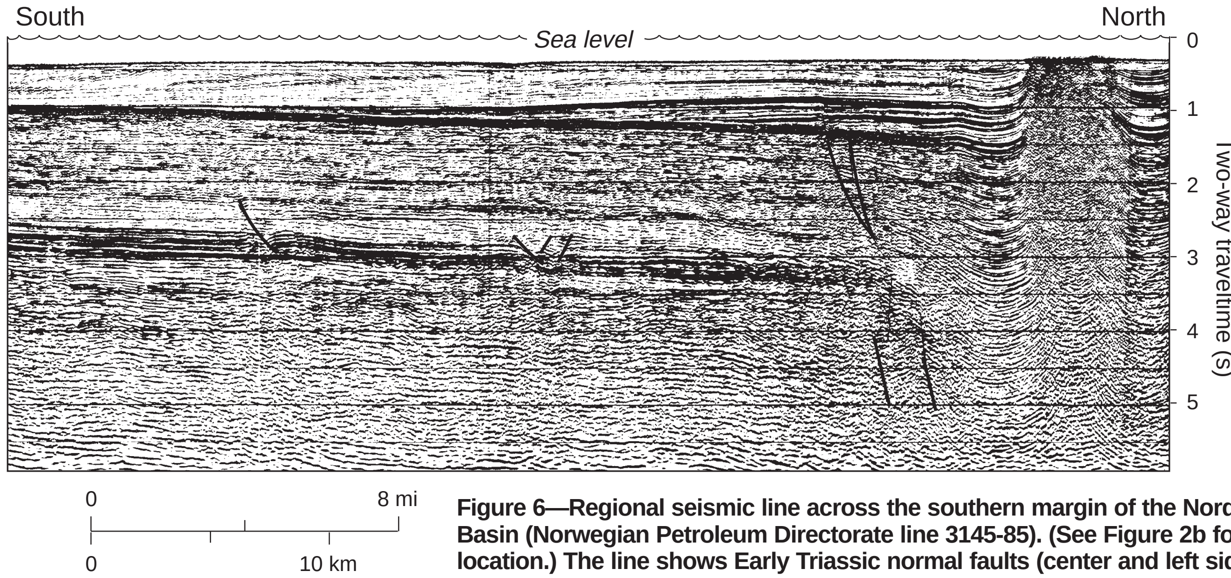

Figure 6—Regional seismic line across the southern margin of the Nordkapp Basin (Norwegian Petroleum Directorate line 3145-85). (See Figure 2b for location.) The line shows Early Triassic normal faults (center and left side) detaching above thin salt.

Gudlaugson et al. (1994) have proposed a more regional model in which the entire Barents shelf subsided and evaporites were deposited in the deep parts of the region. The thickest halite sections were deposited only in the deepest depocenters, such as the Nordkapp Basin. In the Nordkapp Basin itself, the estimates of initial thickness vary from 2.0–2.5 km in the southwestern subbasin to 4.0–5.0 km in the northeastern subbasin (Bergendhal, 1989; Jensen and Sørensen, 1992). The difference in salt thickness between the two subbasins can be attributed to greater basement subsidence in the northeastern than in the southwestern subbasin.

By Late Permian time, the evaporites were overlain by a carbonate section and a Lower Triassic siliciclastic section of relatively uniform thickness (Figures 5, 6), indicating that no significant subsidence occurred in the Nordkapp Basin (Gabrielsen et al., 1992; Jensen and Sørensen, 1992). The evaporitic source layer has long since been depleted by salt flow toward the diapirs, and the presalt, Permian, and Lower Triassic strata are commonly subparallel and tilted toward the basin axis. Sagging of the overburden was caused mainly by salt withdrawal, but faulting and rotation of the subsalt strata suggest that there has been a component of basement subsidence and deepening of the basin during later regional extension.

END OF EARLY TRIASSIC: REGIONAL EXTENSION AND DIAPIRIC INITIATION

Although most authors (e.g., Dengo and Røssland, 1992; Gabrielsen et al., 1992; Jensen and Sørensen, 1992; Koyi et al., 1993; Willoughby and Øverli, 1994) agree on an Early Triassic age for the onset of salt flow, its trigger continues to be debated. Dengo and Røssland (1992) proposed that massive deposition of sediment originating from the Ural Mountains caused differential loading and triggered diapiric rise. However, evidence of Early Triassic collapse of the Urals foreland makes it doubtful that the Urals could have supplied enough sediment to span the rapidly subsiding basin (Dore, 1991). Instead, both seismic and well data point toward the Norwegian mainland, rather than the Ural Mountains, as the main sediment source (Dore, 1991). Our seismic interpretation agrees with the hypothesis of Gabrielsen et al. (1992) that there was no large-scale differential subsidence of the Nordkapp Basin at that time, as indicated by the lack of any significant thickness change in the Lower Triassic sequence (Figures 4, 5, 6).

We agree with the hypothesis of Gabrielsen et al. (1992), Jensen and Sørensen (1992), and Koyi et al. (1993) that diapirs were triggered by normal faulting and thinning of the sediment overburden probably during a phase of basement-involved regional extension that affected the Nordkapp Basin in late Scythian (late Smithian–early Spathian) time. Seismic sections (especially Figure 6) clearly indicate Early Triassic faulting of the Permian and Lower Triassic overburden, and faulting and basinward tilting of the subsalt basement (Figures 4, 5, 6). Moreover, the simultaneous initiation of diapirs in both the northeastern and the southwestern subbasins supports this hypothesis and suggests that the trigger for diapirism was regional tectonics rather than sedimentation. This extensional episode can be correlated with the Variscan–Uralian tectonic phase that affected the Barents Sea area (Dore, 1991; Dengo and Røssland, 1992). Extension triggered diapiric reactive rise (Figure 7), a process described by Vendeville and Jackson (1992a) and Jackson and Vendeville (1994). Normal faulting locally thinned the brittle overburden and created the space necessary for salt to flow upward (Figures 7a, b). Diapirs eventually pierced the thinned graben floors above them (Figure 7c).

Structural clues for this early phase of reactive diapirism are not always visible. Because of subsequent diapiric growth by downbuilding and formation of broad diapir overhangs, normal faults associated with Early Triassic reactive rise, typically located near or against the base of diapir stems, are commonly obscured on seismic reflection data. But evidence for normal faulting can still be found on sections where the structures did not later fully evolve into tall, passive diapirs (right side of Figure 5 and left side of Figure 6). Furthermore, serial seismic sections (Figures 8, 9) illustrate how diapirs connect along strike to salt ridges or pillows overlain by extensional grabens. This geometry is identical to that of scaled models of extensional diapirs that formed first by reactive rise, then grew passively (i.e., by downbuilding) during sedimentation (Vendeville and Jackson, 1992a,b).

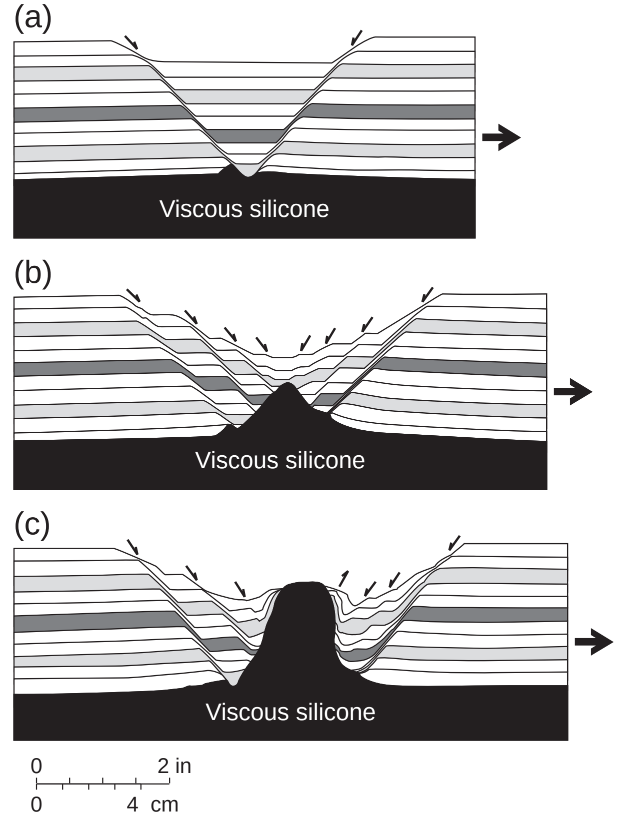

Figure 7—Line drawings of model sections of extensional diapirism. (a) and (b) During the reactive stage, the diapir rose by filling the space created by fault block displacement in the overlying graben. (c) Later, the diapir pierced the thin overburden and rose actively. After Jackson and Vendeville (1994) and Vendeville and Jackson (1992a).

Although Koyi et al. (1993) have proposed that at least some diapirs were originally salt pillows, the relatively uniform thickness of Permian and Lower Triassic strata across the basin suggests that diapirism was triggered by extension rather than by spontaneous rise from salt pillows (as Rayleigh–Taylor instabilities). This is also confirmed by the common lack of rim synclines around many of the Nordkapp Basin diapirs. On most seismic sections, there is no significant change in stratal thickness before active piercement and passive diapiric rise.

Regional extension during the Early Triassic took place at crustal scale and hence deformed basement, salt, and overburden. Therefore, in the Nordkapp Basin, as in the North Sea (e.g., Jenyon, 1986), it is tempting to regard basement faults as triggers for the formation of salt diapirs above. Koyi et al. (1993) suggested that reactivation of basement faults in the Nordkapp Basin has controlled deformation of the salt and its overburden and has localized diapirs above or near the basement faults.

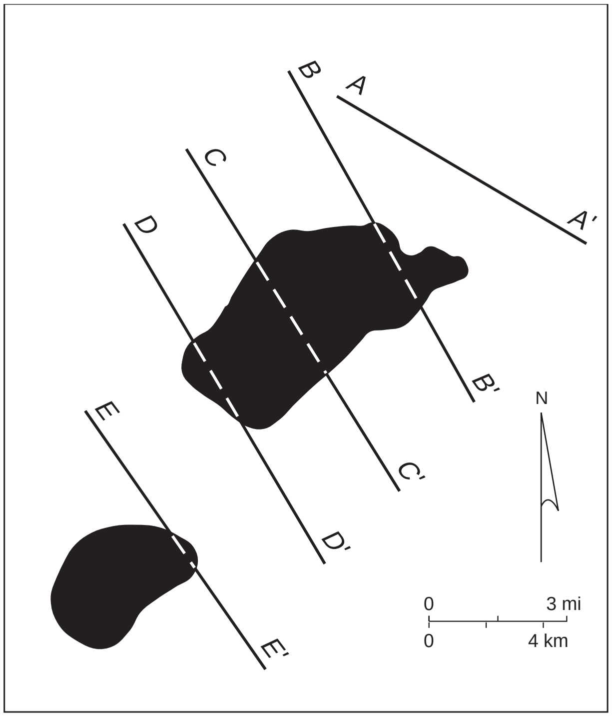

Figure 8—Map (from Geoteam, line NBGS-90) of a salt structure in southwestern Nordkapp Basin. (See Figure 2b for location.) The diapir (black) is shown, along with the location of sections in Figure 9.

However, seismic sections do not show any clear correlation between the location of basement faults and that of the diapirs, suggesting that basement faults and diapirs are not geometrically and genetically related. This conclusion is reinforced by experimental and theoretical work by Vendeville et al. (1993a, 1995). Their results (Figure 10) indicate that the low viscosity of salt rock, combined with the low rate at which crustal extension commonly occurs, means that a thick salt layer acts as a perfect lubricant between its basement and its cover. Deformation localized by faults in the basement is diffused by the thick, weak overlying salt layer rather than being directly transmitted upward through the salt into the overlying sediments.

Because of the large initial salt thickness in the Nordkapp Basin, estimated to be 2–4 km, the source layer acted as a cushion that effectively insulated the sediment overburden from the faulted subsalt basement. Both basement and overburden hence deformed independently (until the source layer had been thinned by salt withdrawal). During thick-skinned extension, diapiric initiation was controlled by overburden thinning (Vendeville et al., 1993a, 1995). The location of the diapirs therefore indicates where overburden grabens, not basement faults, formed in the Early Triassic. As for thin-skinned extension, the location of initial normal faults in the overburden is controlled by various geologic flaws, such as lateral changes in overburden facies or thickness. L. N. Jensen (personal communication, 1994) has suggested

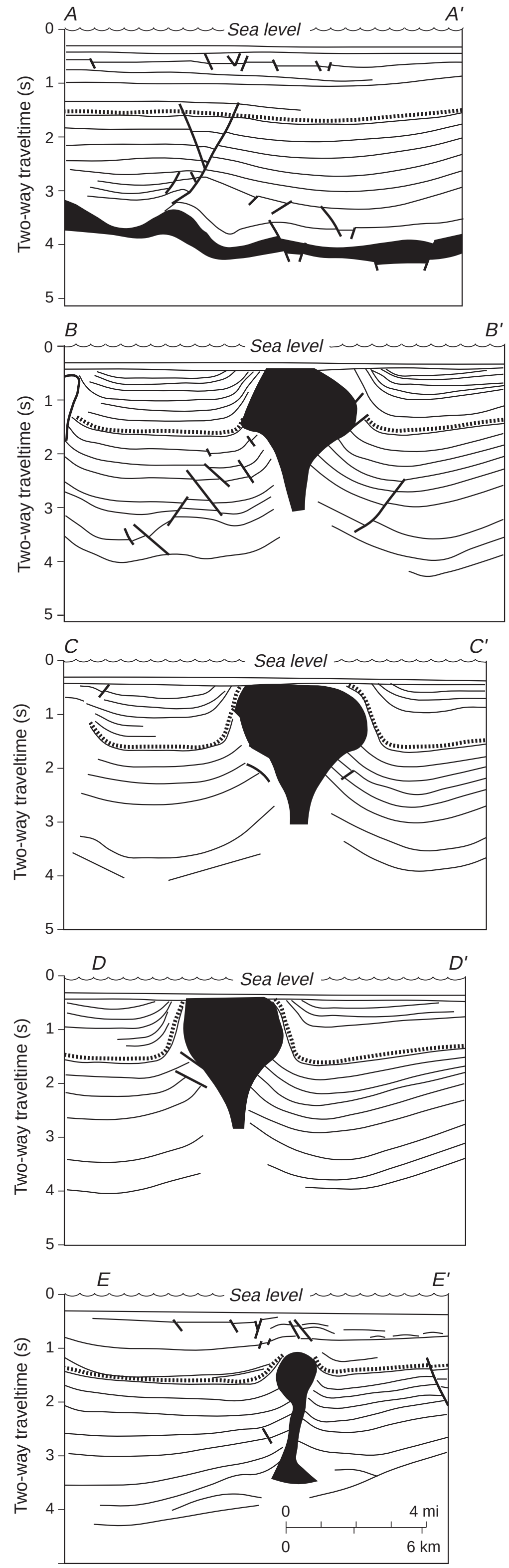

Figure 9—Five serial seismic sections (Geoteam line NBGS-90) cutting across the salt structure in southwestern Nordkapp Basin. (See Figure 8 for locations.) Along strike, the tall diapir in sections B–B' through E–E' becomes a deeply buried salt roller or pillow (section A–A') overlain by an extensional graben.

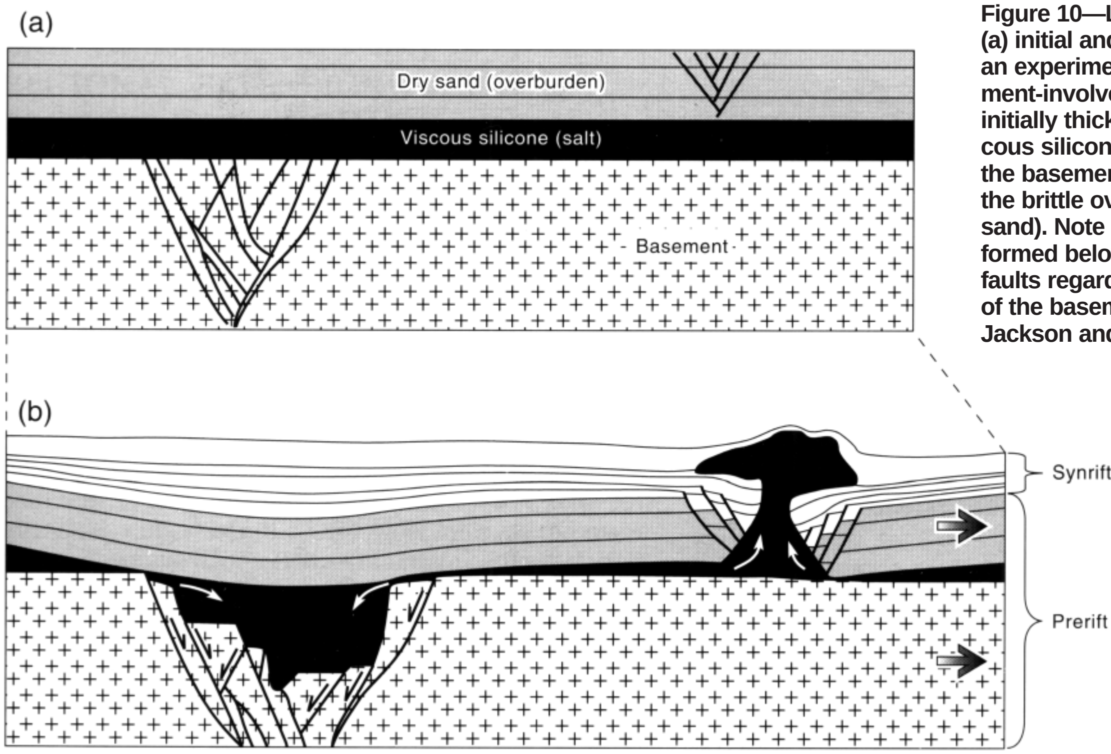

Figure 10—Line drawing of the (a) initial and (b) final stages of an experimental model of basement-involved extension. The initially thick source layer (viscous silicone) fully decoupled the basement (dry sand) from the brittle overburden (dry sand). Note that the diapir formed below the overburden faults regardless of the location of the basement faults. After Jackson and Vendeville (1994).

that asymmetric loading of the salt layer in the Nordkapp Basin by sediments coming from the southeast induced a gentle flexure of the overburden, which in turn forced the Early Triassic overburden faults to initiate preferentially in the center of the basin.

MIDDLE–LATE TRIASSIC: DIAPIRIC GROWTH BY DOWNBUILDING AND GRAVITY GLIDING

Reactive diapirs eventually grew tall enough to actively pierce their thinned roof and emerge at the sea floor (Figure 11). Subsequently, diapirs grew passively by downbuilding, a process described by Nelson (1989, 1991) and Jackson and Talbot (1991), in which diapirs rise by maintaining their crest at or close to the sea floor while sediments accumulate in depotroughs between diapirs. Seismic sections in the Nordkapp Basin indicate that passive growth of diapirs was rapid and salt flow was vigorous. Middle Triassic strata thickened tremendously from the basin margins toward the diapirs (e.g., left side of Figure 11) and formed locally thick wedges that abut against the diapir flank with the apparent geometry of salt rollers. Many of the salt depotroughs are asymmetric. Until Ladinian time, many diapirs in the center of the basin grew with steep or vertical flanks (Figure 11). Some diapirs widened upward during passive growth. This geometry suggests that the rate of net diapiric rise (i.e., vertical salt flow) up the diapir conduit was at least as high as the rate of sediment aggradation in the rapidly subsiding adjacent depotroughs (Vendeville and Jackson, 1991; Vendeville et al., 1993b; Talbot, 1995).

The Anisian marked a significant change in structural style. Although many diapirs continued to grow passively, there is clear evidence that the source layer was thinned or depleted. A major unconformity at the base of the Anisian on seismic sections in the northwestern part of the basin (Figure 12) corresponds to the top Lower Triassic unconformity described by Koyi et al. (1993, their figure 2). Sediments below the unconformity have been strongly deformed and flexed (Figure 12) while the center of the depotroughs was rapidly sinking into the thick salt layer. Sediments on the sides of the depotroughs, being closer to the rising diapirs, were dragged upward by vigorous salt flow and were later truncated by the unconformity. In contrast, sediments above the basal Anisian unconformity (Figure 12) remained largely undeformed, flat-lying, and of uniform thickness. This indicates that, by Anisian time, most overburden depotroughs had grounded onto the subsalt and the source layer had been virtually depleted. Paradoxically, although source layer depletion had restricted or cut off the salt supply, diapirs continued to rise passively after the unconformity episode until Ladinian–Carnian time (Middle Triassic). Seismic sections show that diapirs rose fast enough to even overflow their margins and produce salt overhangs (Figure 13) when the rate of sediment aggradation decreased in Carnian time. The precise geometry and extent of diapir overhangs in the Nordkapp Basin are still debated (Koyi et al., 1992, 1993). Diapir overhangs seem to be larger and more numerous in the northeastern subbasin.

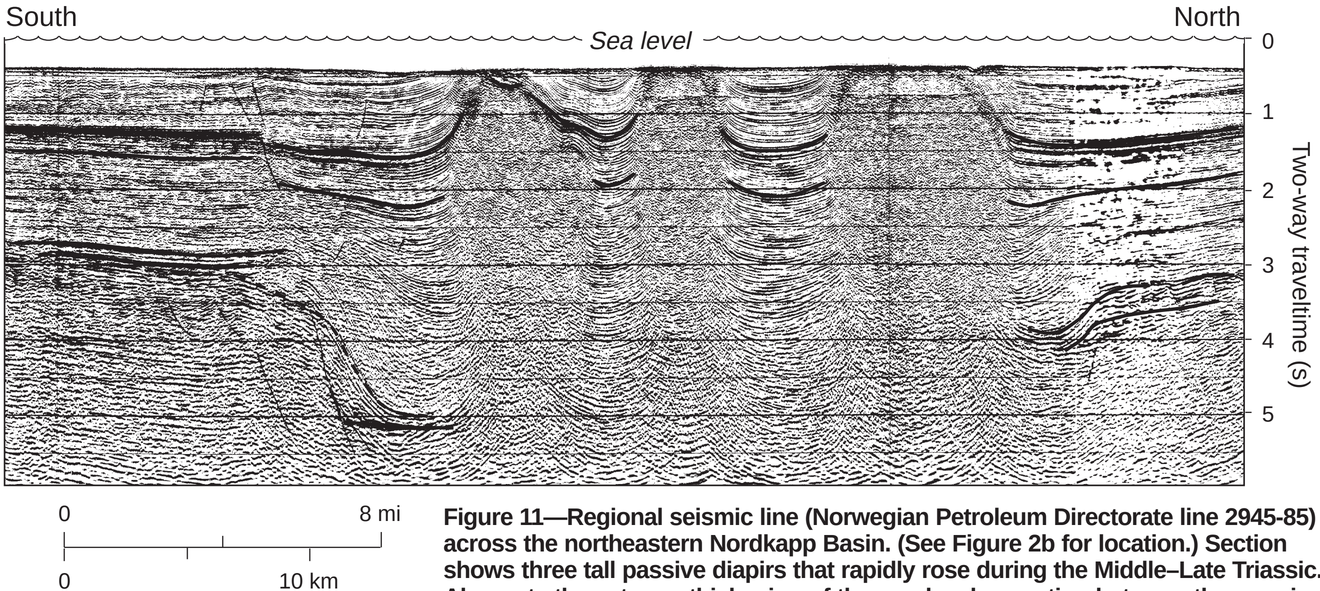

Figure 11—Regional seismic line (Norwegian Petroleum Directorate line 2945-85) across the northeastern Nordkapp Basin. (See Figure 2b for location.) Section shows three tall passive diapirs that rapidly rose during the Middle–Late Triassic. Also note the extreme thickening of the overburden section between the margins and the center of the basin.

Diapiric rise after depletion of its source layer raises both geometrical and mechanical questions. First, there should have been no more salt available to fill the increasing volume of the rising diapirs after Anisian time. Some extra salt could have been squeezed out from under the sides of the depotroughs by flattening the flexed-up base and inverting the depotroughs into turtle structures (as on the Angolan margin; Duval et al., 1992; Lundin, 1992). However, seismic sections in the Nordkapp Basin show no signs of such inversion (e.g., Figures 9, 11, 12, 13). Instead, sediments in the depotroughs seem to have acted as rigid overburden blocks. Second, the mechanical force that drove diapirism during reactive and passive rise could no longer act after the source layer was depleted. As long as the source layer was thick, the increasing weight of sediments in the depotroughs pressurized the salt and forced it to flow laterally from the source layer into the rising passive diapirs. Because the base of the overburden rested directly on the subsalt basement after source layer depletion, thickening of the overburden by sediment aggradation could no longer increase the pressure in the source layer. Therefore, salt flow should have stopped and diapirs should have remained static.

How a diapir can rise without available salt supply from the source layer is illustrated in Figure 14. The basic principle is similar to the mechanism that causes diapiric fall during extension (Vendeville and Jackson, 1992b), but it involves horizontal shortening of the diapir rather than widening. To rise without changing its width, a diapir would have to import more salt to fill the volume increase of the growing diapir (Figure 14b). However, a diapir can rise even without extra salt available if the increase in height is compensated by a decrease in diapir width (Figure 14c). This mechanism is made possible by the overburden blocks behaving far more rigidly than salt.

The applicability of this mechanism was tested using the experimental model shown in Figure 15 (Vendeville, 1993). The model comprised an initially thick source layer of viscous silicone (representing salt) overlain by a brittle sand overburden (representing sediments). The model was first regionally extended during deposition. Extension formed two reactive diapiric ridges that rose below faulted grabens (structures G1 and G2, Figure 15a). Later, the southern segments of the diapiric ridges actively pierced the thin overlying graben floors, emerged at the model surface (structures D1 and D2, Figure 15a), and then grew passively during ongoing extension and deposition. The northern part of the ridges remained in the reactive stage throughout the extensional phase (G1 and G2, Figure 15a).

The experiment was stopped after passive diapirism had largely depleted the source layer and diapiric rise had slowed down. The model was then buried and regionally shortened (Figure 15b). Because viscous silicone is far weaker than sand, the shortening was accommodated by reducing the width of the diapirs, leaving the adjacent overburden blocks virtually undeformed. In the southern part of the model (Figures 15b, c) where diapirs were already at or near the model surface, regional shortening squeezed the silicone out of the diapir stems and forced the diapir to rise. In the northern part of the model (Figures 15b, d) where diapirs were still overlain by a thick roof, shortening flexed the model surface and reactivated some of the old reactive normal faults in reverse slip (Figure 15d). Of particular interest is the absence of obvious signs of shortening in sections where diapirs remained at or near the surface (Figure 15c). Because all the shortening was accommodated by diapiric narrowing rather than by folding or reverse faulting of the adjacent overburden, the diapir in Figure 15c would not be con-

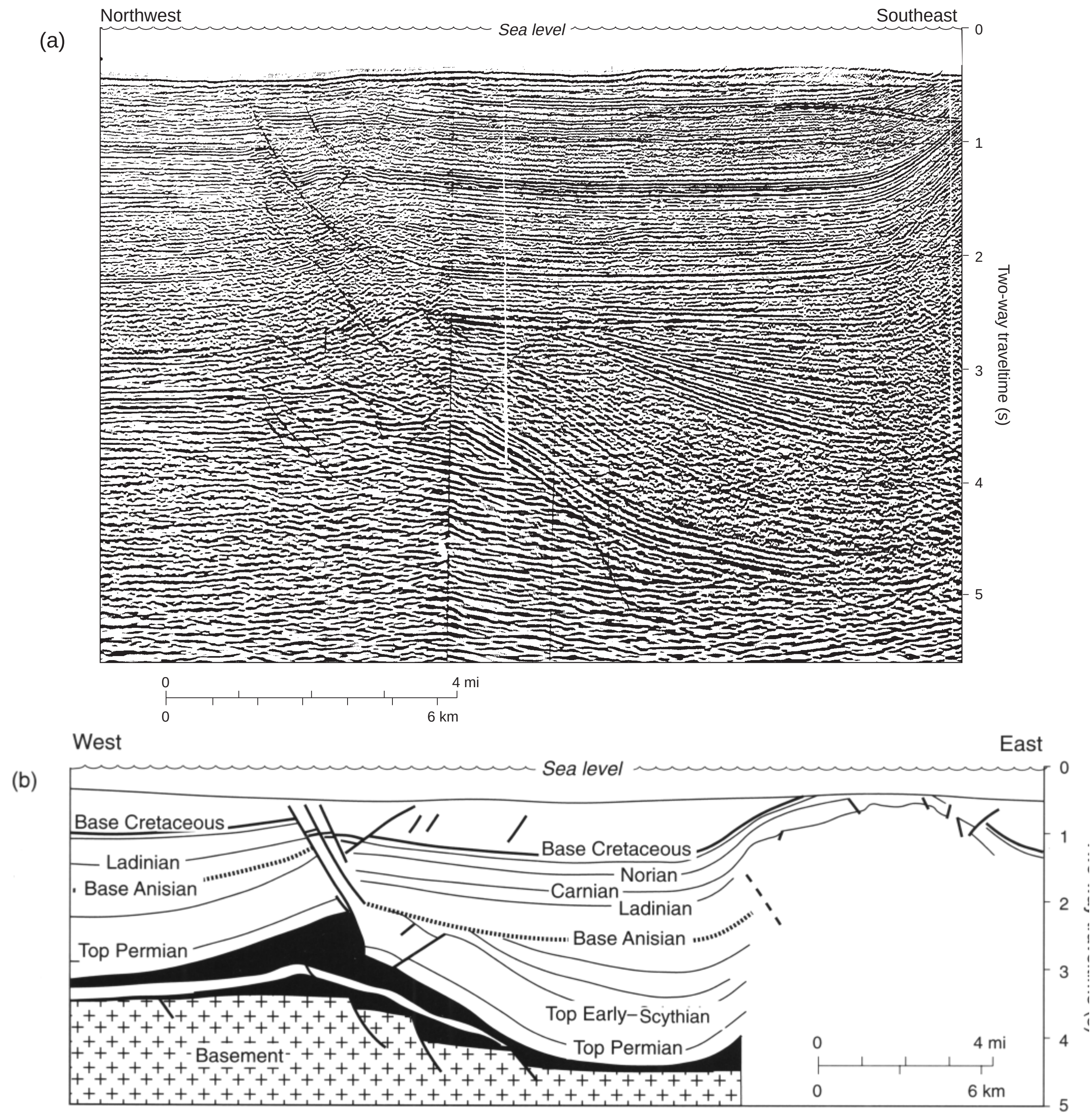

Figure 12—(a) Largely uninterpreted seismic section (Norwegian Petroleum Directorate line D8-85), which forms center-left part of (b) interpreted line drawing showing the change in style of overburden deformation above the Anisian unconformity (hatched line on drawing). (See Figure 2b for location.) Sediments below the Anisian unconformity have been flexed down by salt withdrawal during vigorous diapiric rise. In contrast, sediments above the unconformity are subhorizontal except for drag against the diapir flank and normal faulting on the basin margin.

ventionally interpreted as being driven by shortening. The only indications of diapiric shortening are (1) the evidence for continued diapiric rise after source layer depletion (as in Figure 12) and (2) the reverse faults or folds along strike, where the diapiric ridge had always remained deeply buried.

What caused shortening of the diapirs in the Middle Triassic? We propose that normal displacement along basement faults during an episode of regional extension deepened the basin floor, steepened the basal slope, and triggered down-to-the-basin gravity gliding of sediments above the thinned source layer (Figure 16). This

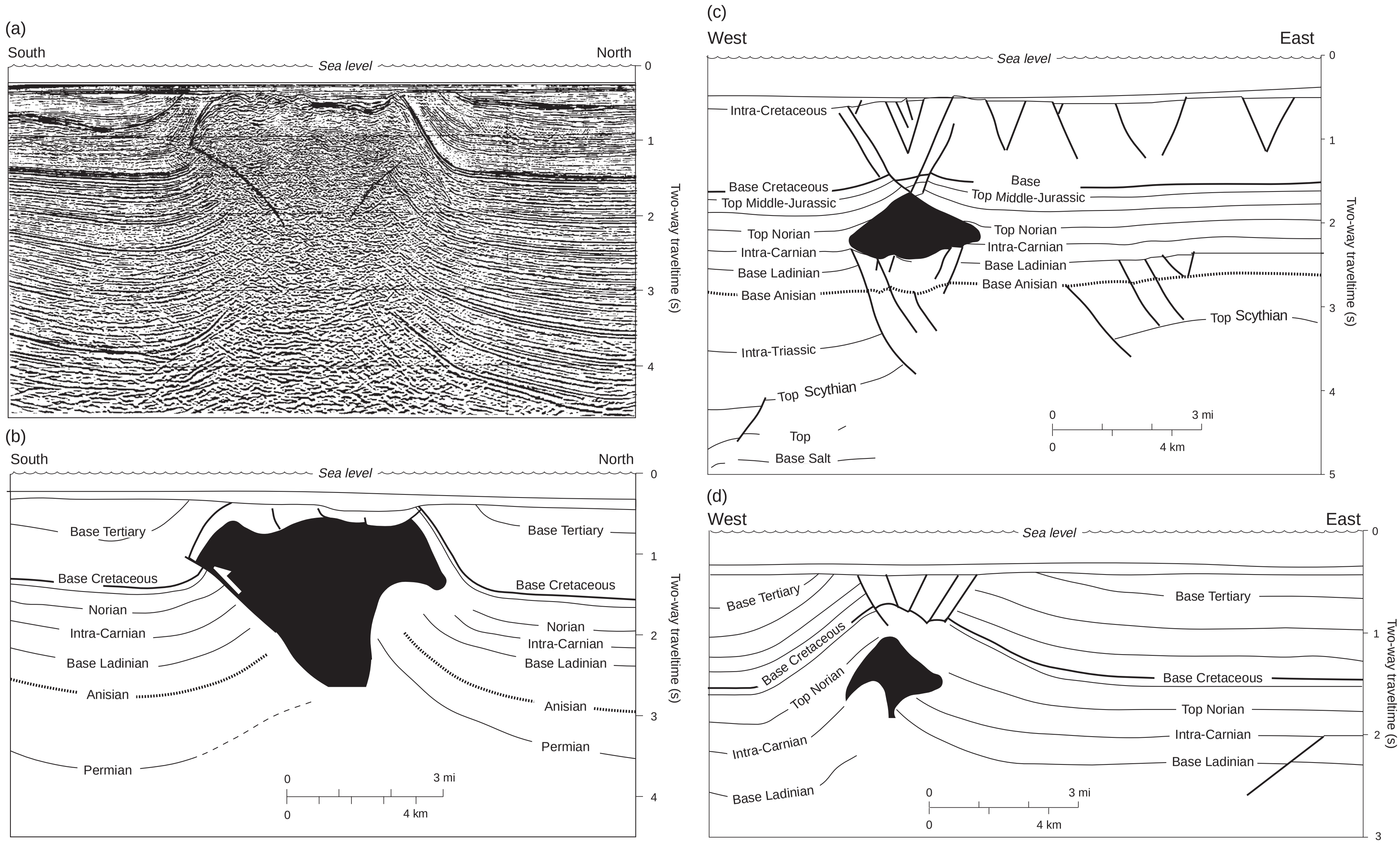

Figure 13—Seismic examples of diapir overhangs emplaced in Ladinian and Carnian time. (a) Uninterpreted seismic section and (b) interpreted line drawing from Geoteam line NBGS-90-209. (c) Interpreted line drawing from Geoteam line NPTN-92-201. (d) Interpreted line drawing from Geoteam line NPTS-92-203. (See Figure 2b for locations.)

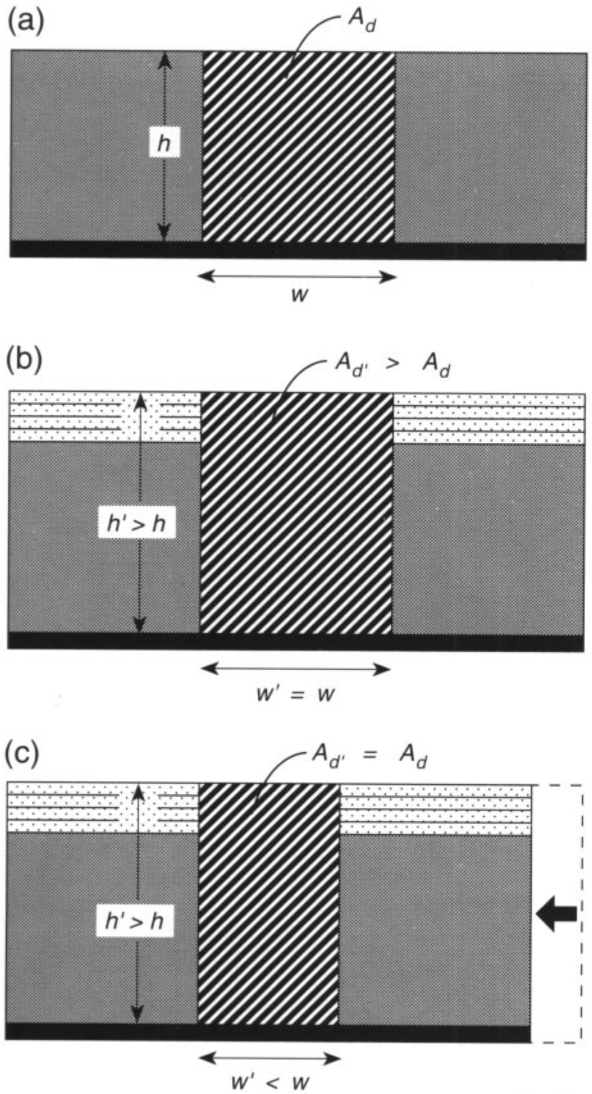

Figure 14—Salt volume problem associated with diapiric growth above a thinned source layer. Black = source layer; striped = diapiric salt. (a) Initial stage with diapiric height = *h*, width = *w*, and salt area in section = A_d. (b) If the diapir grows vertically while maintaining a constant width, *w*, the salt volume A_d must increase to $A_{d'}$ as *h* increases to *h′*. (c) The diapir can grow without a change in salt area, A_d, if its width, *w*, decreases to *w′*.

hypothesis is supported by coeval normal faulting and growth of salt rollers along the basin margins (Figure 4) (Gabrielsen et al., 1992). Steepening of the basin slope caused the overburden blocks to glide downslope under the effect of gravity, squeezing the salt diapirs in the basin center and opening extensional gaps upslope along the basin margin. Because the timing of diapiric growth in Middle–Late Triassic time remains strikingly similar across the Nordkapp Basin (e.g., diapirs formed overhangs in Carnian time in both the northeast and southwest subbasins), we advocate that gravity gliding was triggered by regional tectonics that steepened the slope, rather than by more local influences. Thus, during Middle–Late Triassic time, regional extension tightly controlled diapiric growth, albeit indirectly by triggering gravity gliding. Without regional extension and deepening of the basin, diapirs in the Nordkapp Basin would have stopped rising as early as the onset of Anisian time when salt withdrawal had already depleted the source layer.

By Late Triassic, the diapirs stopped rising and were buried. Although widespread block faulting occurred throughout the western Barents Sea in Late Jurassic–Early Cretaceous time (Brekke and Riis, 1987; Gabrielsen et al., 1990, 1992; Dengo and Røssland, 1992), it does not seem to have significantly affected the Nordkapp Basin, except for the southernmost part (Krokan, 1988; Bergendahl, 1989). In the rest of the basin, the only visible effect of this block faulting was a minor pulse of active diapiric rise recorded by a slight thinning of Upper Jurassic strata against the diapir flanks. The diapirs were then buried under 1000–1500 m of flat-lying Cretaceous sediments. That diapirs were then extinct is clearly demonstrated by the fact that sedimentary wedges prograded without interruption across the basin above the diapir crests (Figures 6, 17). If the diapirs had been active, they would have deformed the sea floor topography, which would have affected or retarded progradation of the wedges. Such wedges were later deformed by diapiric rejuvenation during Late Cretaceous–middle Tertiary time.

LATE CRETACEOUS: DIAPIRIC REACTIVATION BY GRAVITY GLIDING

Another episode of diapiric rise occurred during the Late Cretaceous. Although many structural clues in the upper part of the sedimentary cover were later removed by Pliocene–Pleistocene erosion (1000–1200 m of sediments removed) (Nyland et al., 1992; Riis, 1992; Vågnes et al., 1992), the Cretaceous episode of active diapirism is clearly visible on most seismic sections in the Nordkapp Basin (Figures 6, 11, 13, 17, 18). Active diapirs rose above the regional datum by arching their thick roofs. Most sections show diapir roofs containing grabens at their crest and monoclinal folds above diapir shoulders. A few sections (Figure 19) show synthetic reverse faults on the side of the uplifted roof that are similar to those formed in experimental models of active diapirism (Vendeville and Jackson, 1992a; Schultz-Ela et al., 1993). In the southwestern subbasin, the diapir crests were eroded. In addition, mound-like and fan-like deposits can be interpreted as the result of mass flows triggered by subsidence. Their age has been interpreted by Henriksen (1990) and Henriksen and Vorren (in press) as early Tertiary, but correlation with nearby wells suggests that their age is Late Cretaceous. The timing for diapiric reactivation also neatly coincides with Late Cretaceous rifting of the North Atlantic (Faleide et al., 1993; Hinz et al., 1993, Knott et al., 1993). This tectonic episode is known to have affected the western Barents Sea, producing associated salt tectonics in the Tromsø and Sørvestsnaget basins (Faleide et al., 1993).

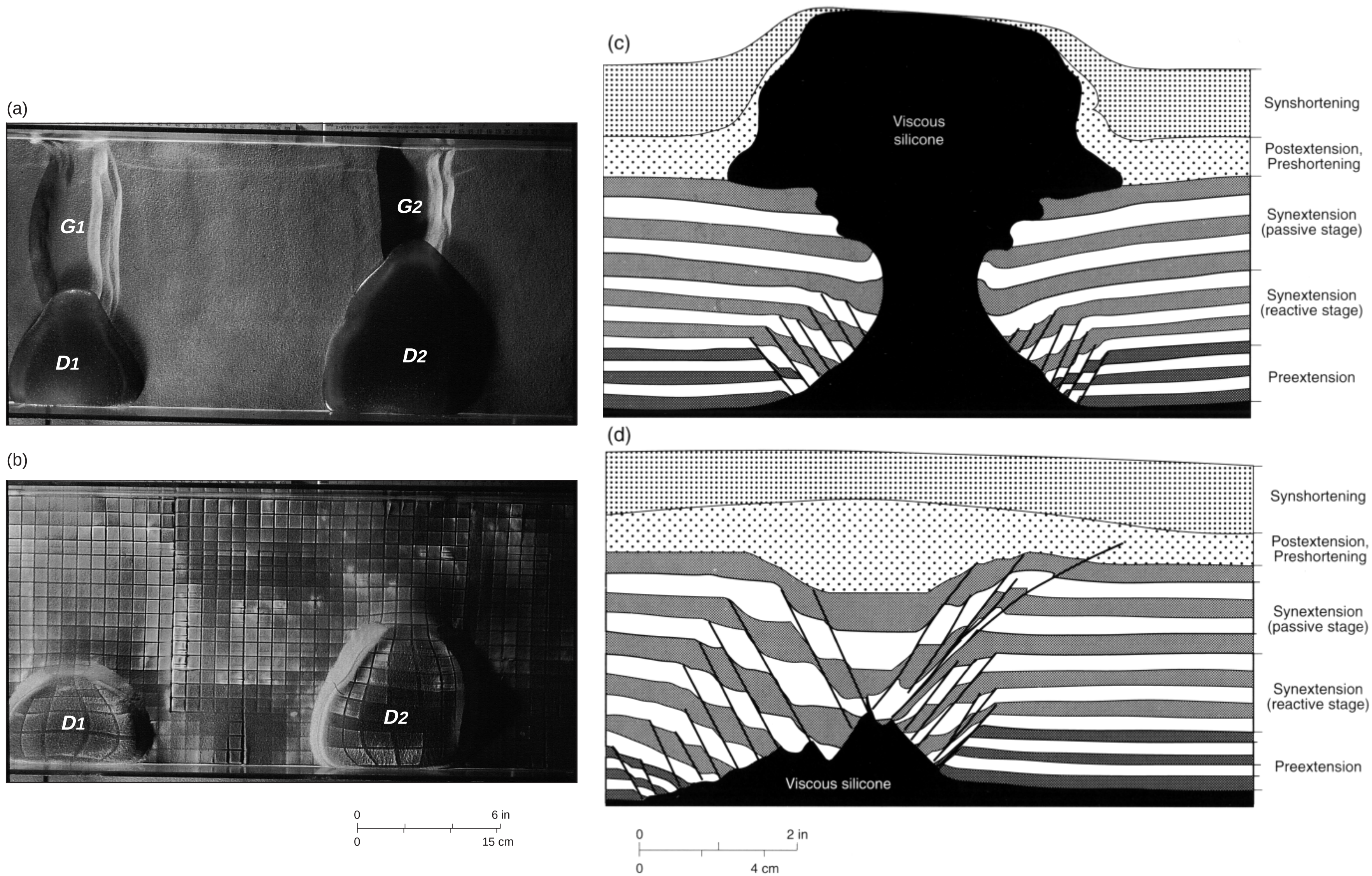

Figure 15—Experimental model of early extension and diapirism followed by regional shortening. (a) Overhead view of model following early extension. Extension produced two grabens (G1 and G2) below which diapirs rose reactively. Rounded diapirs (D1 and D2) later actively pierced the southern part of the model grabens, then grew passively. (b) Overhead view of model following burial and late shortening. Grid lines are passive markers printed on the model surface. The old passive diapirs (D1 and D2) were reactivated during shortening and rose actively, while stretching and distorting their thin roof. Northern part of the model shows little evidence of shortening. (c) Cross section of the southern part of the model, where diapirs had emerged before shortening. Section shows the old normal faults formed during the reactive stage, stratigraphic thickening during the passive stage, and bending of the diapir roof during late shortening and vertical rise. There are no folds or reverse faults in the adjacent overburden. (d) Cross section of the northern part of the model, where diapirs had remained in the reactive stage before shortening and always had a thick roof. Late shortening deformed the structure by anticlinally warping the model surface and reactivating some of the old normal faults as reverse faults.

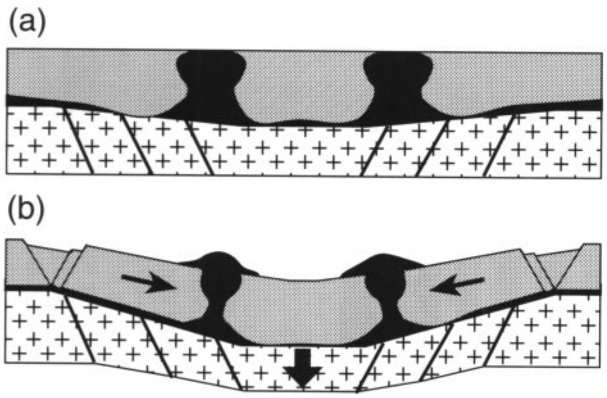

Figure 16—Schematic diagrams illustrating how basement subsidence during crustal extension deepens the basin, steepens the basin slopes, and triggers down-to-the-basin gravity gliding. This induces shortening of the diapirs in the basin center and normal faulting on the margins.

Following the hypothesis of Rønnevik (1982) that the Late Cretaceous regional extension had reactivated structures in the Nordkapp Basin, we propose that regional extension triggered down-to-the-basin gravity gliding and reactivated the diapirs. The mechanism causing diapiric rise is similar to that of the Middle–Late Triassic episode illustrated in Figures 14 and 16, except that diapirs were overlain by a thick roof prior to the Late Cretaceous gravity gliding and renewed rise. Unlike spontaneous active diapirism, which is driven by pressure differences in a thick source layer and can easily be prevented by a thick roof (Vendeville and Jackson, 1992; Schultz-Ela et al., 1993), diapiric reactivation by local shortening after source layer depletion was driven by the slope-parallel component of the weight of the entire overburden blocks between the basin margin and the diapirs in the basin center. This process pressurizes the diapir and can easily overcome the strength of even a thick overburden roof. Our hypothesis that Late Cretaceous diapiric reactivation was driven by gravity gliding is supported by coeval extensional faulting along the basin margins, which created the Nysleppen, Måsøy, and Thor Iversen fault complexes (Gabrielsen et al., 1990). Gabrielsen et al. (1990) also described reverse faults of Late Cretaceous age above a salt pillow (Figure 4b, bottom left) and suggested that the margins of the basin were compressed. However, we have interpreted such apparent reverse faults as Early Triassic normal faults that were later rotated passively during Late Cretaceous subsidence and basement tilting.

We conducted a second set of experiments (Figure 20) to test the applicability of this mechanism and to investigate the deformation style above circular and linear salt structures during late shortening. For simplicity, diapirs were triggered purely by sedimentary differential loading. An initially thick source layer of viscous silicone was overlain by a thin sand layer of uniform thickness. Deformation started after we vacuumed six holes in the sand layer (two linear and four circular; see location and shape in Figure 20a). The viscous silicone rose diapirically through the holes, forming passive diapirs that maintained their crest at the model surface during subsequent deposition of new sand layers. The diapirs rose passively until source layer depletion caused them to stop growing. We buried the then-inactive diapirs under a 2-cm-thick

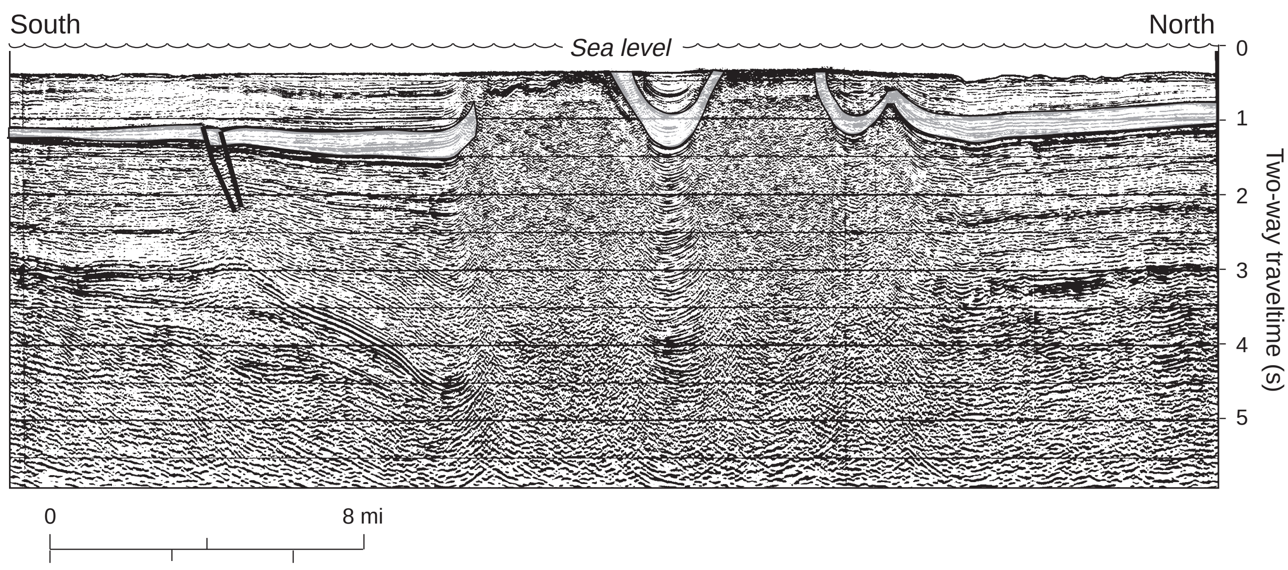

Figure 17—Regional seismic section across the northeastern subbasin (Norwegian Petroleum Directorate line 3115-85) showing a Lower Cretaceous sediment wedge (gray; also visible in Figure 6) that prograded southward across the basin above the then inactive diapirs. The wedge was later deformed during Late Cretaceous and middle Tertiary diapiric reactivation. (See Figure 2b for location.)

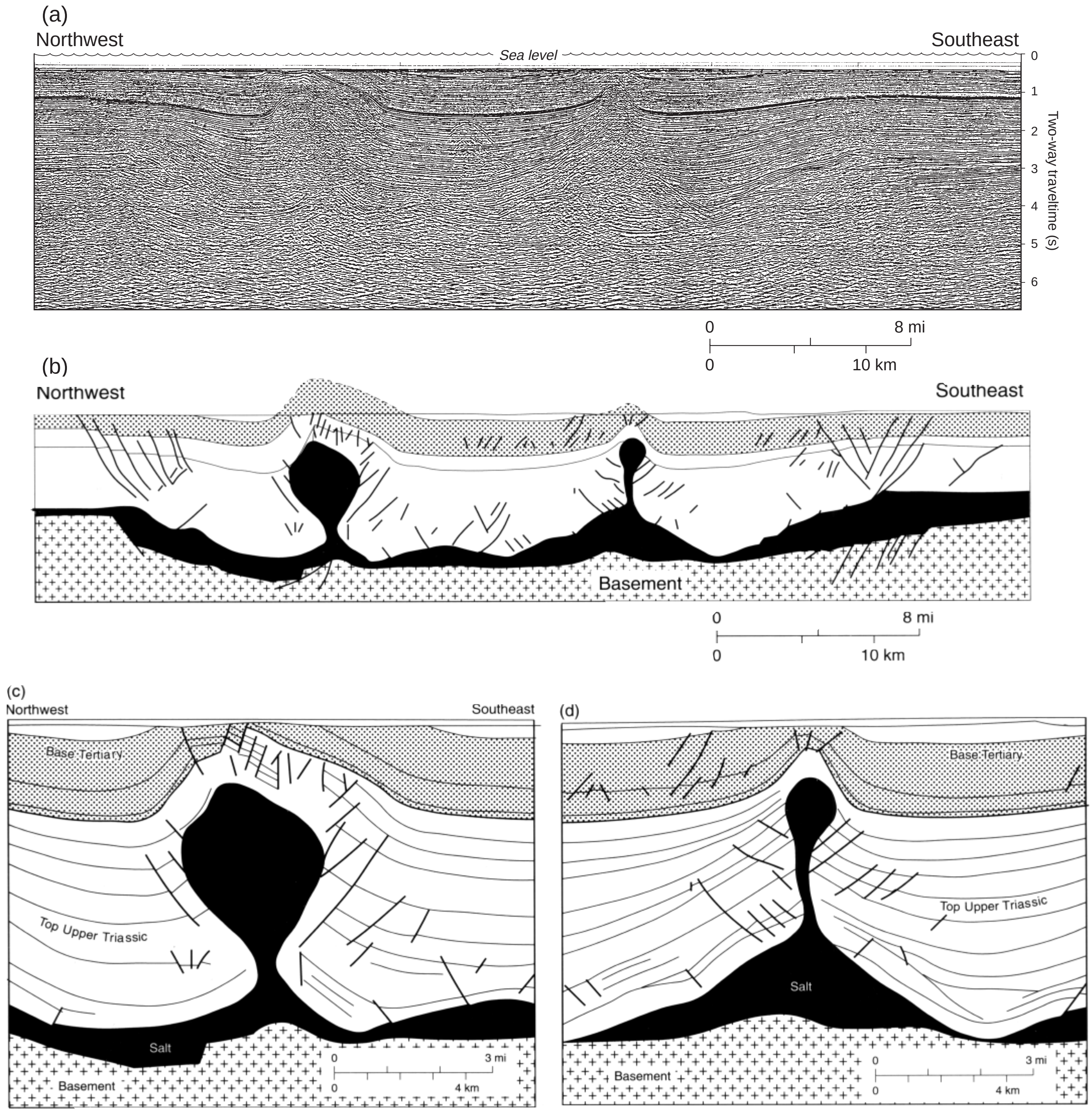

Figure 18—(a) Regional time-migrated seismic line across the southwestern subbasin. (b) Line drawing of depth-converted section. (c) and (d) Details of diapirs in this section, also depth converted. No vertical exaggeration. Sections show that Jurassic and Cretaceous sediments (top stippled layer) of regionally uniform thickness were deformed by active rise in the Late Cretaceous and middle Tertiary. (See Figure 2b for location.)

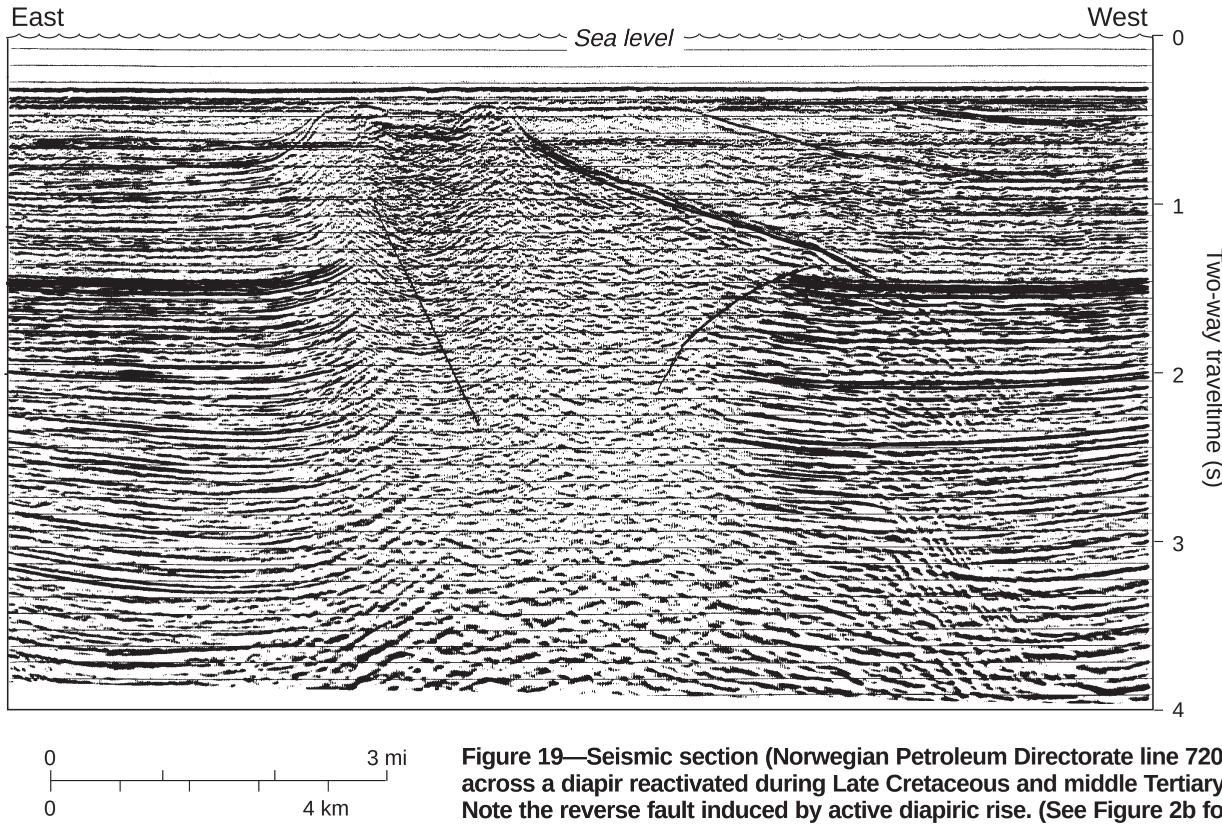

Figure 19—Seismic section (Norwegian Petroleum Directorate line 720730-86) across a diapir reactivated during Late Cretaceous and middle Tertiary time. Note the reverse fault induced by active diapiric rise. (See Figure 2b for location.)

sand layer (representing the 1000–1500 m of uniformly thick Cretaceous sediments in the Nordkapp Basin; lightly stippled in Figure 20c,d) and regionally shortened the entire model.

An overhead view of the model after shortening (Figure 20b) shows that most diapirs were reactivated during shortening. Diapirs rose by lifting their thin roofs, forming crestal grabens (diapirs 5, 6, 7 in Figure 20b) and flexing the sediments above the diapir shoulders. The traces of the crestal normal faults are not consistently oriented with respect to the direction of regional shortening. Instead, fault traces appear to follow the shape of the diapir in planform, indicating that the horizontal component of stretching of the diapir roof caused by diapir rise far outweighed the horizontal component due to regional shortening. In other words, the height of most diapirs increased much faster than their width decreased. Two squeezed diapirs (diapirs 3 and 4 in Figure 20b) even emerged at the surface and formed new overhangs. We attribute the rapid diapiric rise to the fact that they were initially tall and narrow prior to regional shortening. Tall, narrow diapirs rise vigorously in response to a small amount of shortening (Figure 21, left side). Their deformation style is thus closer to that of structures formed purely by vertical diapiric rise than that of structures formed by regional shortening. In contrast, initially low, wide diapirs (Figure 21, right side) do not rise as much, and their deformation style is closer to that typical of regional shortening.

Because most diapirs in the Nordkapp Basin had initially narrow stems, the deformation style of their roofs is similar to that above vertically rising diapirs (Figures 22, 23). Around some of the model diapirs (see large north-trending fault trace east of diapirs 4 and 5 in Figure 20b), the flexure above the diapir shoulders was tight enough to initiate shallow reverse faults. Sections in the model (Figure 20c) indicate that such shallow reverse faults are similar to those above active diapirs (Vendeville and Jackson, 1992a; Schultz-Ela et al., 1993) and are not caused directly by regional shortening. These shallow reverse faults commonly root at depth onto the top of the diapir or at the tip of diapir overhangs. The model showed only one large, through-going reverse fault (southwest corner of Figure 20 B, near diapir 7) that can unmistakably be interpreted as a direct result of regional shortening. In the rest of the model, regional shortening was entirely accommodated by laterally squeezing the diapirs, forcing them to rise.

Model sections (Figures 20c, d) and seismic examples from the Nordkapp Basin (Figures 22, 23, 24) illustrate the difficulty of finding evidence of shortening in areas where most of the deformation was accommodated by narrowing the diapirs. Sections cutting across diapirs (Figures 20c, 23a, b) typically show no signs of shortening and display only active diapirs. The only clues that could lead an interpreter to suspect that shortening has occurred are mechanical. That diapirs would have actively risen again after depleting their source layer, would

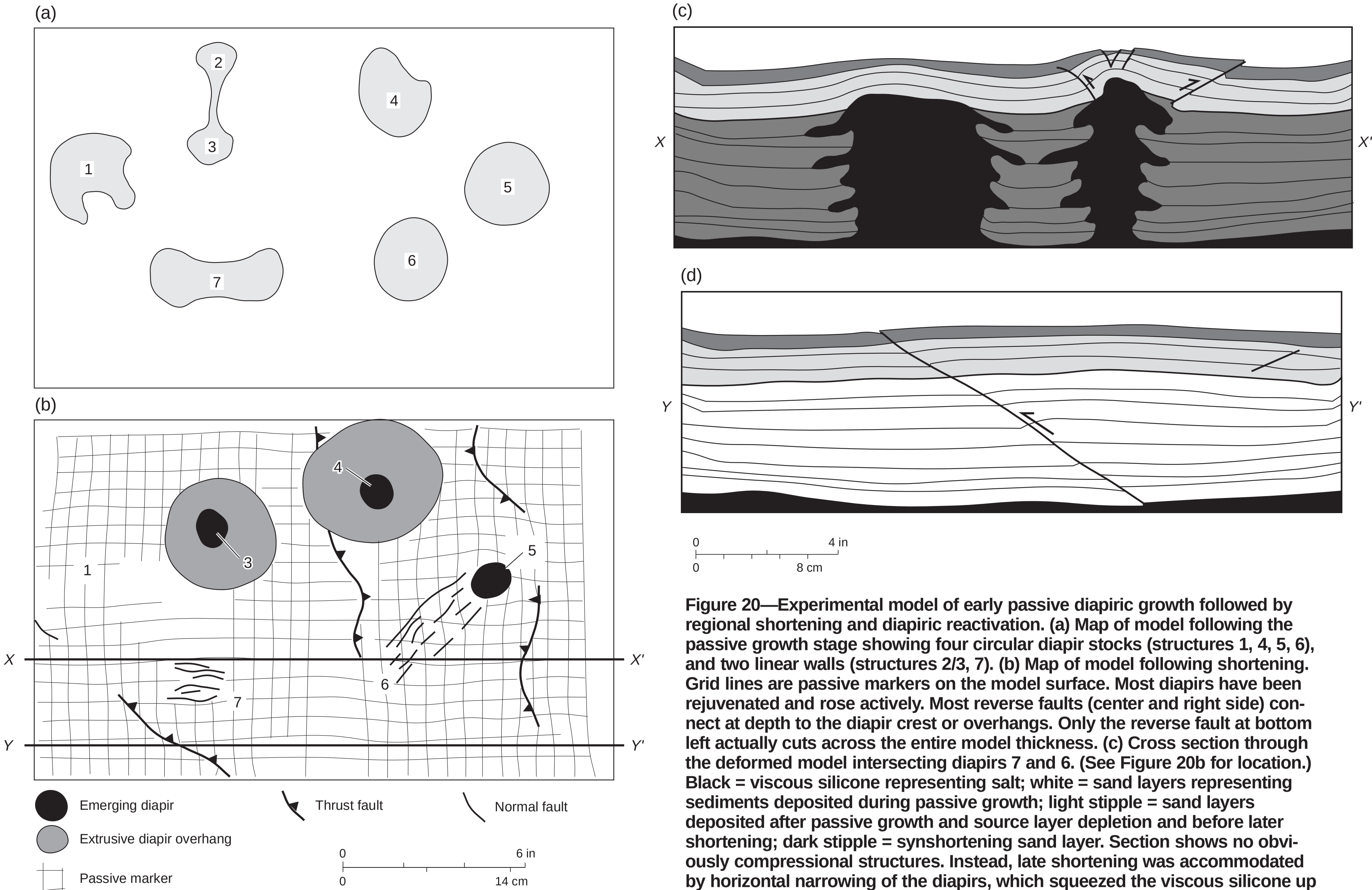

Figure 20—Experimental model of early passive diapiric growth followed by regional shortening and diapiric reactivation. (a) Map of model following the passive growth stage showing four circular diapir stocks (structures 1, 4, 5, 6), and two linear walls (structures 2/3, 7). (b) Map of model following shortening. Grid lines are passive markers on the model surface. Most diapirs have been rejuvenated and rose actively. Most reverse faults (center and right side) connect at depth to the diapir crest or overhangs. Only the reverse fault at bottom left actually cuts across the entire model thickness. (c) Cross section through the deformed model intersecting diapirs 7 and 6. (See Figure 20b for location.) Black = viscous silicone representing salt; white = sand layers representing sediments deposited during passive growth; light stipple = sand layers deposited after passive growth and source layer depletion and before later shortening; dark stipple = synshortening sand layer. Section shows no obviously compressional structures. Instead, late shortening was accommodated by horizontal narrowing of the diapirs, which squeezed the viscous silicone up and out of the stems. This forced diapirs to rise actively and deform their thick roofs. (d) Cross section not intersecting diapirs. The large reverse fault cutting through the entire section accommodated the late shortening.

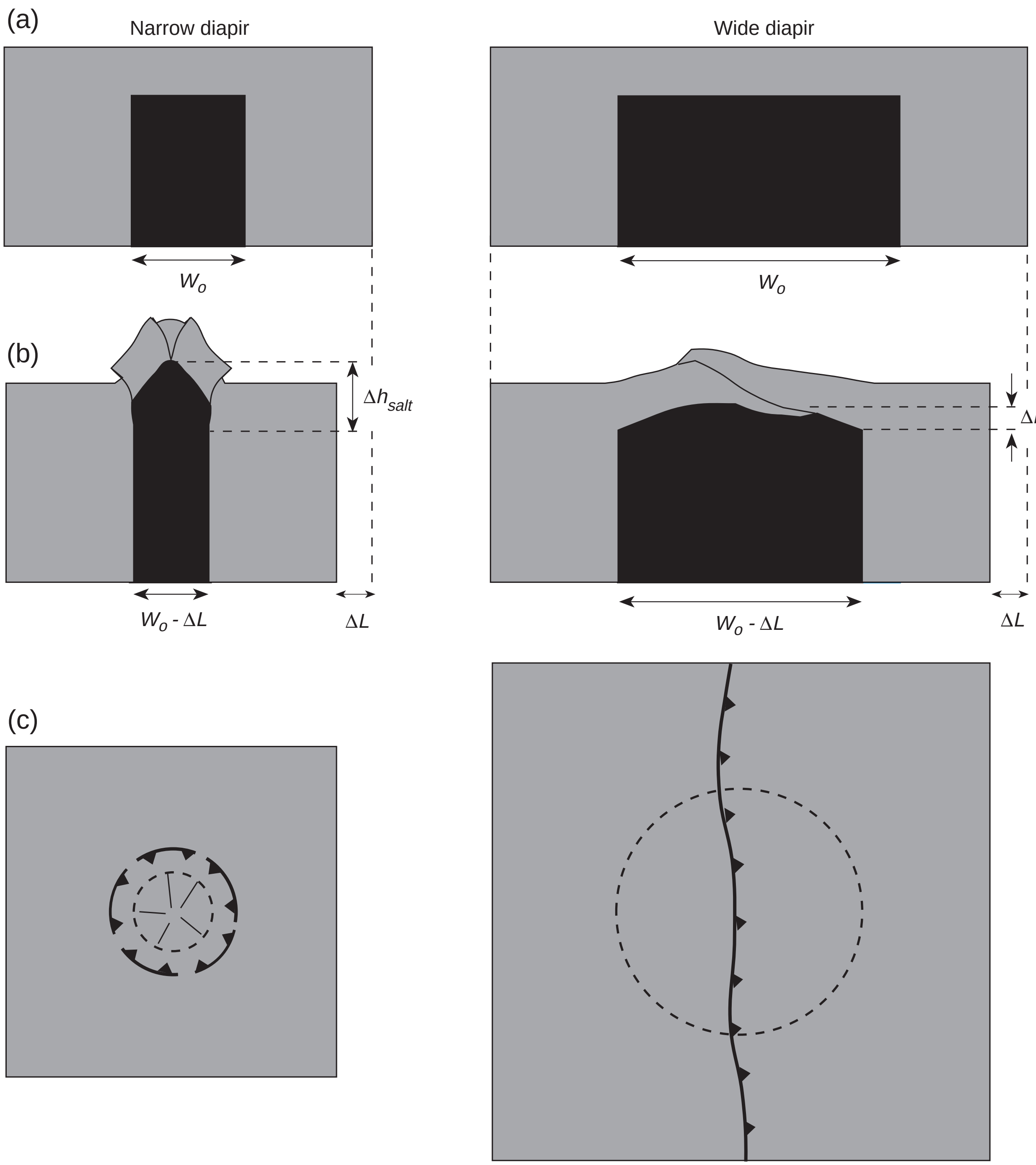

Figure 21—Conceptual diagram illustrating how (a) initially tall and narrow diapirs (left column) (b) rise higher and faster than initially wide and stocky diapirs (right column) for the same amount of horizontal shortening, ΔL. The increase in diapiric height, Δh_{salt}, depends on the initial diapiric width, W_o, and on the component of horizontal shortening, ΔL. Because the vertical displacement, Δh_{salt}, during reactivation of narrow diapirs largely exceeds the component of horizontal shortening, ΔL, the deformation style is that of a vertically rising active diapir. (c) Normal and reverse faults above narrow diapirs follow the diapiric shape regardless of the direction of regional shortening (left side). In contrast, the component of horizontal shortening, ΔL, during reactivation of wide diapirs exceeds the vertical displacement, Δh_{salt}. The deformation style is thus closer to that of regional compression, and the diapir forms only a slight topographic bulge that does not significantly disturb the local stress field. Reverse faults do not necessarily follow the diapiric shape but can form perpendicular to the direction of regional shortening (right side).

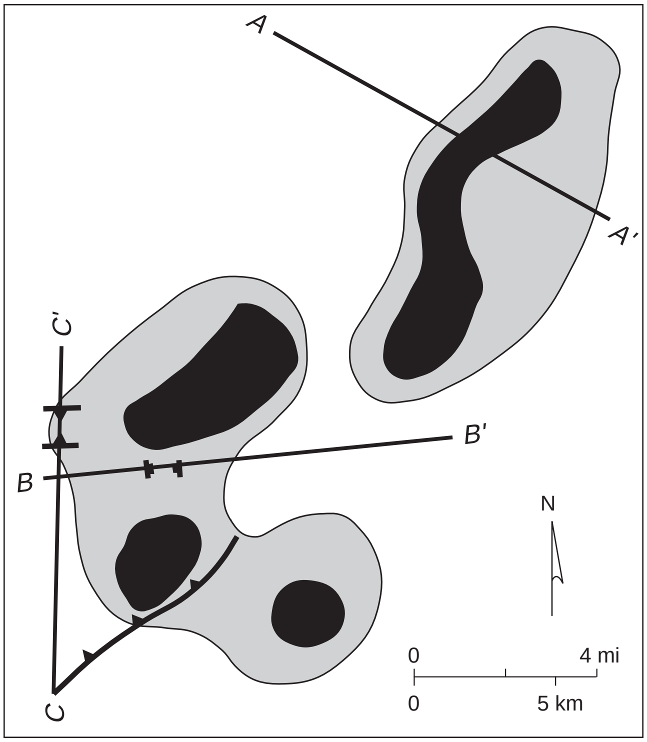

Figure 22—Map of salt diapirs reactivated by shortening in southwestern Nordkapp Basin. (See Figure 2b for location.) Locations of the seismic sections in Figure 23 are shown. Black = diapirs close to the Pliocene–Pleistocene erosion surface; stippled = base of the Cretaceous sediments uplifted above regional datum.

have stopped growing for a long time, and would then have been buried under a thick roof implies that there was an external trigger. Another clue can be found by looking for contractional structures in sections along strike that do not cut across diapirs.

In the experiment, the section in Figure 20d shows a large reverse fault that cuts across the entire overburden section and therefore must have been induced by regional shortening rather than by vertical diapiric rise. In the seismic example, only sections away from the diapir stems (Figures 23c, 24) show folding and reverse faulting associated with shortening of the central part of the basin. The last clue for late-stage diapiric shortening is the shape of the diapir stem in planform. Assuming that diapirs had circular planforms before shortening, their planforms should have become elliptical after diapiric narrowing (Figure 25), with the short axis parallel to the direction of maximum shortening. The Nordkapp Basin comprises many salt diapirs whose stems are elliptical (Figure 26). Although the elliptical shape might have been partially inherited from older reactive salt ridges during Late Triassic extension, it also reflects later shortening.

The Late Cretaceous pulse of active diapiric rise ended, and diapirs were buried under 1500 m of lower Tertiary sediments.

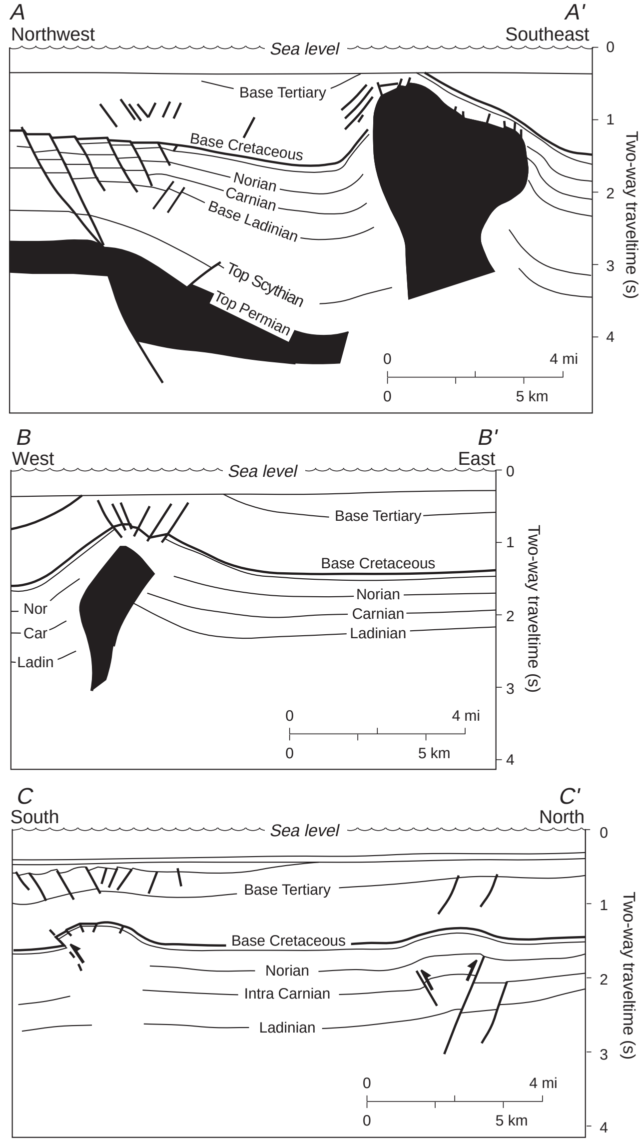

Figure 23—Interpreted line drawings of seismic sections located in Figure 22. Sections A–A' (Geoteam line NBGS-90-423) and B–B' (Geoteam line NBGS-90-203) cut across preexisting diapirs, thus no obviously contractional structure is visible. Instead, shortening was accommodated mostly by narrowing of the diapir stems. Note the nearly complete pinch-off of the diapir stem on section B–B'. Section C–C' (Geoteam line NPTS-92-301) is away from the diapir stems and shows reverse faults and folds caused by Late Cretaceous and middle Tertiary shortening that was accommodated elsewhere by diapiric narrowing.

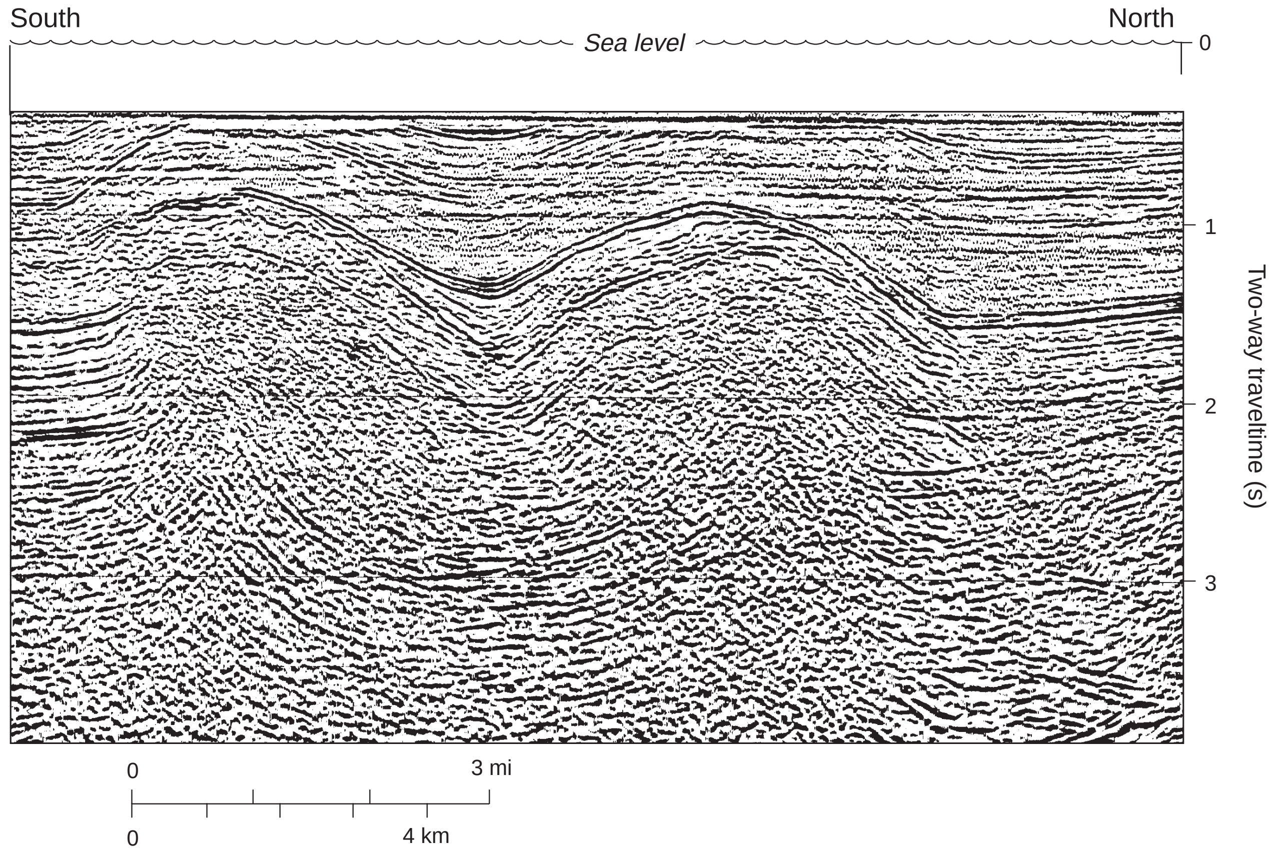

Figure 24—Seismic section (Norwegian Petroleum Directorate line 2700-87) located away from diapir stems. Like section C–C' in Figure 23, this section shows reverse faults and folds caused by Late Cretaceous and middle Tertiary shortening. (See Figure 2b for location.)

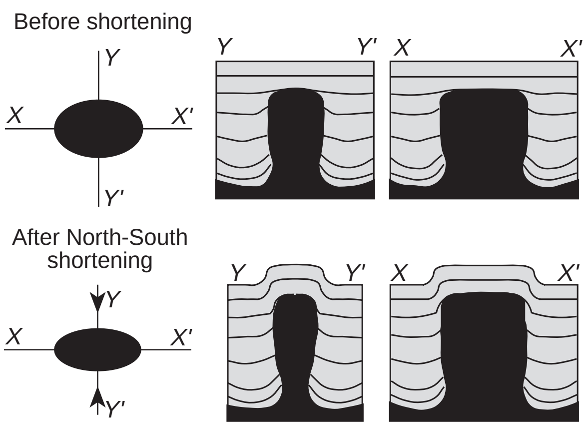

Figure 25—Conceptual diagram showing the change in planform (left) and vertical sections (right) of a diapir reactivated by late shortening. The initially elliptical diapiric planform is deformed into an even tighter ellipse after north-south shortening. Sections normal to the direction of shortening (section X–X') show no change in diapiric width. On section Y–Y', parallel to the direction of regional shortening, the diapiric width has decreased. (See Figure 26 for examples of this concept.)

MIDDLE TERTIARY: DIAPIRIC REACTIVATION BY REGIONAL SHORTENING

In the middle Tertiary (Eocene–Oligocene), a new regional tectonic event (described by Brekke and Riis, 1987; Gabrielsen and Faerseth, 1988; Gabrielsen et al., 1990; Dengo and Røssland, 1992; Riis and Fjeldskar, 1992; Sales, 1992; Nilsen, 1994; Reemst et al., 1994) triggered the last phase of diapiric rise in the Nordkapp Basin. Unlike the Middle–Late Triassic and Late Cretaceous phases, no normal faulting along the basin margin was associated with the middle Tertiary diapiric rise. Instead, because the base of the Cretaceous in some sections is slightly warped above the regional datum along the basin margin (Figure 27), we infer that middle Tertiary diapiric growth was not induced by gravity gliding triggered by regional extension but instead by regional contraction in the Nordkapp Basin. At the scale of the diapirs, deformation was very similar to that during the Late Cretaceous. Diapirs responded to horizontal shortening by rising vertically and lifting and fracturing their roofs. This last episode of horizontal shortening pinched off the stem of many diapirs, giving them a tear-drop geometry.

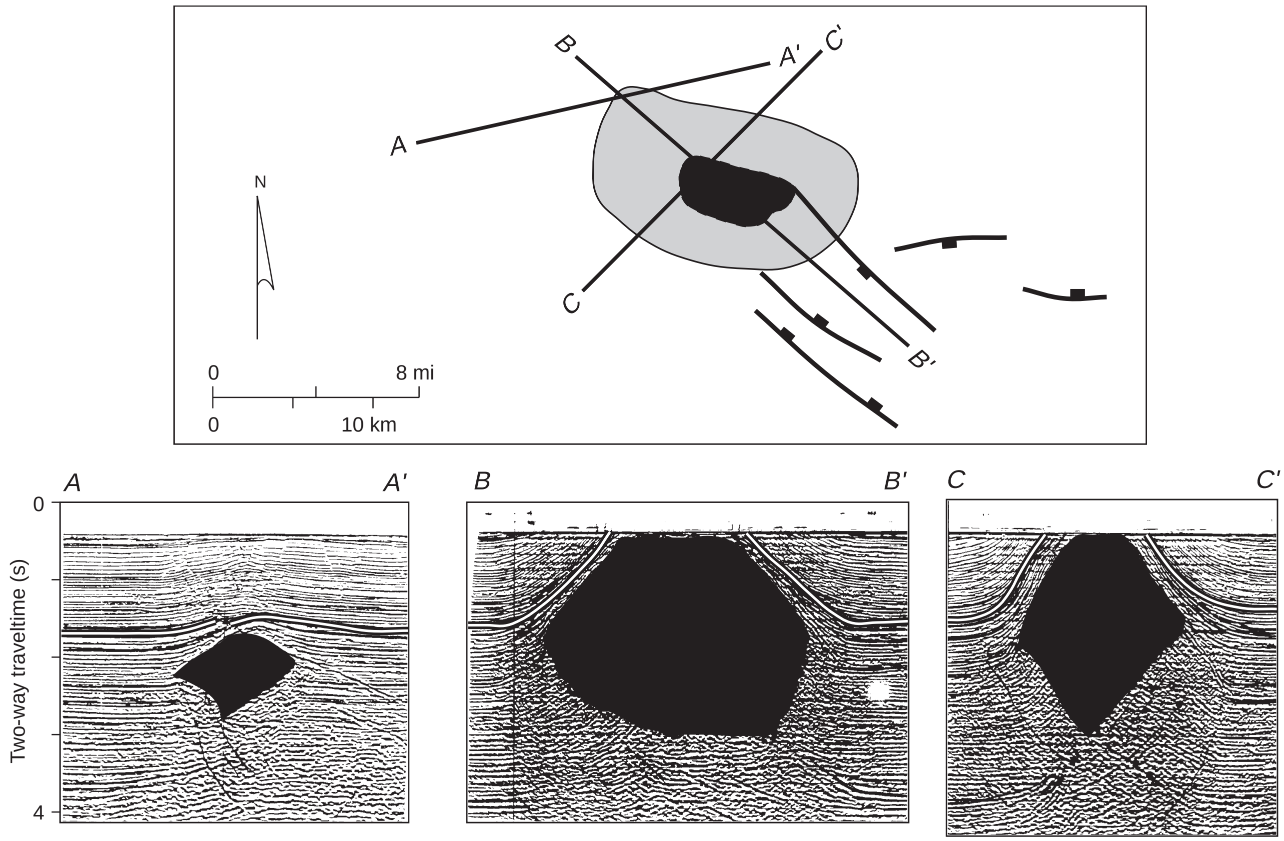

Figure 26—Seismic examples from the Nordkapp Basin illustrating the concept shown in Figure 25. (See Figure 2b for locations.) Section A–A' is Geoteam line NPTN-92-201. The diapir stem is much narrower in section C–C' (Geoteam line NPTN-92-407) than in B–B' (Geoteam line NPTN-92-210).

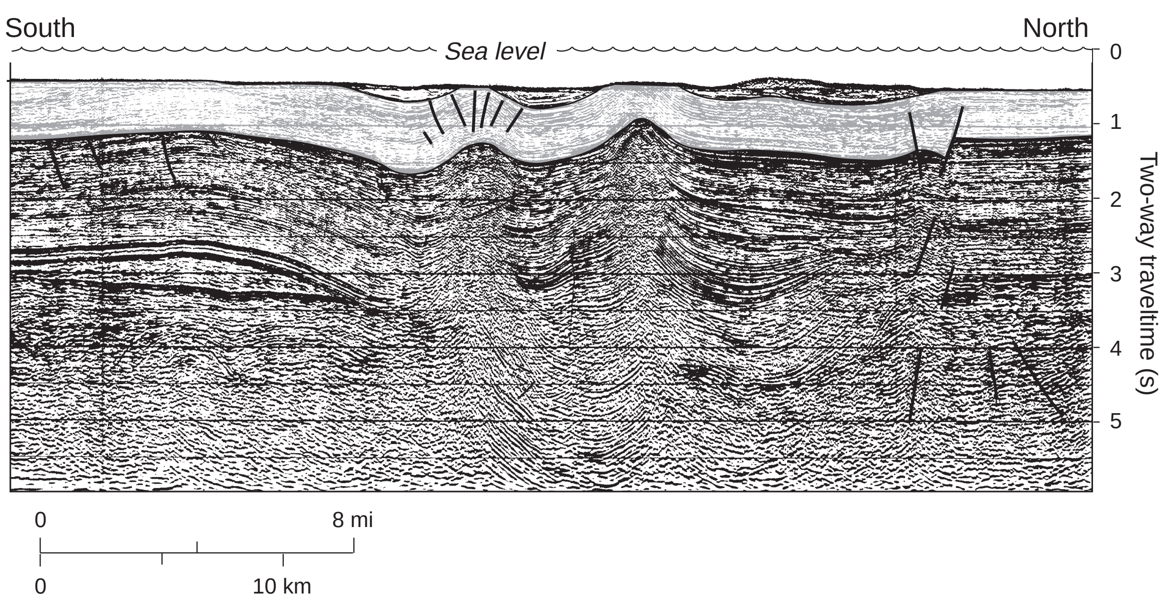

Figure 27—Regional seismic line across the northeastern subbasin (Norwegian Petroleum Directorate line 2845-85) showing Cretaceous sediments (gray) deformed during diapiric rejuvenation in the Late Cretaceous and middle Tertiary (open folds in the center of basin). In contrast, the broad fold on the south margin of the basin (left side) was directly caused by middle Tertiary regional compression. (See Figure 2b for location.)

In models simulating a fluid overburden, tear-drop diapirs are interpreted as very mature diapirs that formed by Rayleigh–Taylor instability in which salt rises buoyantly and eventually pinches off the initially wide stems by deforming the adjacent viscous overburden. In the examples illustrated here, stem pinch-off was neither induced by buoyancy forces, nor did it occur by deforming the adjacent overburden. Salt was expelled upward under the lateral pressure of the rigid, undeformed overburden blocks. The driving force was not imposed by the salt diapir itself but was either the slope-parallel component of the weight of the overburden gliding downslope or simply horizontal regional compression. Because many of the depotroughs had acquired a concave-upward base during downbuilding in Triassic time, the diapirs were usually wider at their base than higher up in the section. When shortening in Late Cretaceous and middle Triassic time closed the diapirs at their narrowest width, it commonly left a small, triangular pedestal of remaining salt at the diapir base (Figures 18c, d). Koyi et al. (1992) attributed this apparent geometry to a velocity pull-up effect caused by overlying diapir overhangs. However, the presence of such triangular pockets of salt at the base of diapirs devoid of overhangs (e.g., Figure 18d) indicates that they are real structures and not mere seismic artifacts.

No diapiric activity occurred after the middle Tertiary pulse. The Barents Sea strata were subsequently uplifted during the Pliocene–Pleistocene and were deeply eroded. Erosion is thought to have removed more than 1000 m of sediments in the Nordkapp Basin (Eidvin and Riis, 1989; Riis and Jensen, 1992; Vågnes et al., 1992; Reemst et al., 1994). The area then subsided and was overlain by thin (100–200 m) Pleistocene sediments; the sea floor is now below 300–400 m of water. The diapirs now have negligible bathymetric expression.

CONCLUSIONS

The evolution of salt structures was once commonly regarded as depending mainly on the intrinsic properties of salt and overburden rocks, such as density contrast, viscosity difference, and initial thicknesses. The geometry and growth rate of salt diapirs were believed to be controlled much more by these parameters than by external processes such as regional tectonics. Our observations in the Nordkapp Basin suggest that halokinesis can be intimately and primarily controlled by regional tectonics. In the Nordkapp Basin, diapirs did not rise continually through geologic time. Rather, they grew by short pulses separated by long periods of inactivity. Each burst of diapiric rise can be chronologically and genetically tied to an episode of regional tectonics in the Barents Sea area. Early Triassic regional extension triggered the onset of diapirs by fracturing and thinning their overburden. Middle–Late Triassic regional extension and basin subsidence allowed the diapirs to keep growing even after they had depleted the source layer. Another episode of gravity gliding during Late Cretaceous basement-involved extension reactivated the diapirs. Finally, middle Tertiary compression triggered the last episode of diapiric rise in the basin.

In this chapter, we have presented a new process of diapiric reactivation in which regional extension deepens the basin floor, steepens the basal slope, and triggers gravity gliding. This has induced normal faulting on the basin margin and lateral contraction and renewed diapiric growth in the basin center. We think this process is also applicable to diapirs in other salt basins. For example, diapirs at the base of the slope in the Gulf of Mexico have pinched-off stems and had their last surge of vertical rise during an episode of local shortening. We have also described a new mode of diapir stem pinch-off, a feature encountered on many seismic sections. This process operates when local shortening squeezes initially wider, preexisting diapirs and pinches off their stems, without requiring any significant strain of the rigid adjacent overburden blocks.

Acknowledgments *We thank Geoteam, Geco-Prakla and their partners (Esso, Norsk Hydro, and Statoil) , and the Norwegian Petroleum Directorate for allowing us to use and reproduce seismic data. The experimental modeling was conducted at the Applied Geodynamics Laboratory, Bureau of Economic Geology, The University of Texas at Austin, with funds from the Texas Advanced Research Program and the following companies: Agip S.p.A, Amoco Production Company, Anadarko, ARCO Exploration and Production Technology, BP Exploration Inc., Chevron Petroleum Technology Company, Conoco Inc., Exxon Production Research Company, Louisiana Land and Exploration, Marathon Oil Company, Mobil Research and Development Corporation, Petroleo Brasileiro S.A., Phillips Petroleum Company, Société National Elf-Aquitaine Production, Statoil, Texaco Inc., and Total Minatome Corporation. We thank Bobby Duncan, Martin Jackson, Tucker Hentz, Jake Hossack, Lars Jensen, Hemin Koyi, and Dave Roberts for comments on the manuscript, and Michele Bailey for drawing the figures. Special thanks to Beth Dishman and Dottie Johnson for their patience in handling countless phone calls between Norway and Texas during this research.*

REFERENCES CITED

Bergendhal, E., 1989, Halokinetisk utvikling av Nordkapp-bassengets sørvestre segment: Master's thesis, University of Oslo, Norway, 120 p.

Brekke, H., and F. Riis, 1987, Tectonics and basin evolution of the Norwegian shelf between 62°–72°: Norsk Geologisk Tidsskrift, v. 67, p. 295–322.

Bruce, J. R., and D. F. Toomy, 1993, Late Paleozoic biotherm occurrences of the Finnmark shelf, Norwegian Barents Sea: analogues and regional significance, *in* T. Vorren, ed., Arctic geology and petroleum potential: London, Elsevier, p. 377–392.

Dengo, C. A., and K. G. Røssland, 1992, Extensional tectonic history of the western Barents Sea, *in* R. M. Larsen et al., eds., Structural and tectonic modelling and its application to petroleum geology: Norwegian Petroleum Society Special Publication, p. 91–107.

Dore, A. G., 1991, The structural foundation and evolution of Mesozoic seaways between Europe and Arctic: Paleogeography, Paleoclimatology, Paleoecology, v. 87, p. 441–492.

Duval, B., C. Cramez, and M. P. A. Jackson, 1992, Raft tectonics in the Kwanza basin: Marine and Petroleum Geology, v. 9, p. 389–404.

Eidvin, T., and F. Riis, 1989, Nye dateringer av de tre vestlige borehullen i Barentshavet. Resultater og konsekvenser for den tertiaere hevningen: Norwegian Petroleum Directorate Bulletin No. 27, 44 p.

Faleide, J. I., S. T. Gudlaugson, and G. Jacquart, 1984, Evolution of the western Barents Sea: Marine and Petroleum Geology, v. 1, p. 120–150.

Faleide, J. I., E. Vågnes, and S. T. Gudlaugson, 1993, Late Mesozoic–Cenozoic evolution of the southwestern Barents Sea, *in* J. R. Parker, ed., Petroleum geology of northwest Europe: Proceedings of the Fourth Conference, Geological Society of London, p. 933–950.

Gabrielsen, R. H., and R. R. Faerseth, 1988, Cretaceous and Tertiary reactivation of master fault zones of the Barents Sea: Norsk Polar Institute Report No. 46, p. 93–97.

Gabrielsen, R. H., R. R. Faerseth, L. N. Jensen, J. E. Kalheim, and F. Riis, 1990, Structural elements of the Norwegian continental shelf, part I, the Barents Sea region: Norwegian Petroleum Directorate Bulletin No. 6, 33 p.

Gabrielsen, R. H., O. S. Kløvjan, and T. Stølan, 1992, Interaction between halokinesis and faulting: structuring of the margins of the Nordkapp Basin, Barents Sea region, *in* R. M. Larsen et al., eds., Structural and tectonic modelling and its application to petroleum geology: Norwegian Petroleum Society Special Publication, p. 121–131.

Gerard, J., and C. Buhrig, 1990, Seismic facies of the Barents shelf: analysis and interpretation: Marine and Petroleum Geology, v. 7, p. 234–252.

Gudlaugson, S. T., J. I. Faleide, S. E. Johansen, and A. Breivik, 1994, Late Paleozoic structural development of the southwestern Barents Sea, *in* S. E. Johansen, Geological evolution of the Barents Sea with special emphasis on late Paleozoic development: Ph.D. dissertation, University of Oslo, Norway, 46 p.

Henriksen, S., 1990, Den Kenozoiske utvikling av det sørvestlige Nordkappbasenget: Master's thesis, Institute for Biologi og Geologi, Uitø, 168 p.

Henriksen, S., and T. O. Vorren, in press, Early Cenozoic sequence stratigraphy and salt tectonics in the Nordkapp Basin: Norsk Geologisk Tidsskrift

Hinz, K., O. Eldholm, M. Block, and J. Skogseid, 1993, Evolution of North Atlantic volcanic continental margins, *in* J. R. Parker, ed., Petroleum geology of northwest Europe: Proceedings of the Fourth Conference, Geological Society of London, p. 901–914.

Jackson, M. P. A., and C. J. Talbot, 1991, A glossary of salt tectonics: The University of Texas at Austin, Bureau of Economic Geology Geological Circular 91-4, 44 p.

Jackson, M. P. A., and B. C. Vendeville, 1994, Regional extension as a geologic trigger for diapirism: GSA Bulletin, v. 106, p. 57–73.

Jensen, L. N., and K. Sørensen, 1992, The tectonic framework and halokinesis of the Nordkapp Basin, Norwegian Barents Sea, *in* R. M. Larsen et al., eds., Structural and tectonic modelling and its application to petroleum geology: Norwegian Petroleum Society Special Publication, p. 109–120.

Jensen, L. N., K. Sørensen, K. Kåsli, O. Riise, and J. R. T. Granli, 1993, Regional assessment and palinspastic restoration of halokinesis in the Nordkapp Basin, Barents Sea (abs.): AAPG, International Hedberg Research Conference Abstracts, Sept. 13–17, Bath, U.K., p. 99.

Jenyon, M. K., 1986, Salt tectonics: London, Elsevier, 191 p.

Johansen, S. E., B. K. Ostisky, Ø. Birkeland, Y. F. Federovsky, V. N. Martirosjan, B. Christensen, S. I. Cheredeev, E. A. Ignatenko, and L. S. Margulis, 1993, Hydrocarbon potential in the Barents Sea region: play distribution and potential, *in* T. O. Vorren et al., eds., Arctic geology and petroleum potential: Elsevier, Norwegian Petroleum Society, p. 273–320.

Johansen, S. E., T. Henningsen, E. Rundhoude, B. M. Sather, C. Fichler, and H. G. Rueslåtten, 1994, Continuation of the Caledonides north of Norway: seismic reflectors within the basement beneath the southern Barents Sea: Marine and Petroleum Geology, v. 11, p. 190–201.

Karpaz, M. R., O. Roberts, V. Moralev, and E. Terekhov, 1993, Regional lineament framework of eastern Finnmark, Norway, western Kola Peninsula, Russia and southern Barents Sea: Proceedings of the Ninth Thematic Conference on Geological Remote Sensing, Pasadena, California, p. 733–750.

Kjøde, J., K. M. Storetvedt, O. Roberts, and A. Gidskehaüg, 1978, Paleomagnetic evidence for large-scale dextral movement along the Trollfjord-Komagelu fault, Finnmark north Norway: Physics of Earth and Planetary Interiors, v. 16, p. 132–144.

Knott, S. D., M. T. Burchell, E. J. Jolley, and A. J. Fraser, 1993, Mesozoic to Cenozoic plate reconstruction of the North Atlantic and hydrocarbon plays of the Atlantic margins, *in* J. R. Parker, ed., Petroleum geology of northwest Europe: Porceedings of the Fourth Conference, Geological Society of London, p. 953–974.

Koyi, H., S. Nybakken, K. Hogstad, and B. Tørrudbakken, 1992, Determining geometry of salt diapirs by depth modeling of seismic velocity pull-up: Oil and Gas Journal, October 5, p. 97–101.

Koyi, H., C. J. Talbot, and B. Tørrudbakken, 1993, Salt diapirs of the southwest Nordkapp Basin: analogue modelling: Tectonophysics, v. 228, p. 167–187.

Krokan, B., 1988, Et gravimetrisk studium av Nordkappbassenget: Master's thesis, Institute for Geology, University of Oslo, Norway, 174 p.

Lippard, S., 1994, Permo-Carboniferous basaltic dykes and fault systems on Magerøya; some new observations and implications for rifting in the southern Barents Sea (abs.): Tectonic and structural geology studies group meeting on reactivation of offshore and onshore basement structures, Norwegian Geological Society, Tromsø, Norway, Nov.

Lundin, E. R., 1992, Thin-skinned extensional tectonics on a salt detachment, northern Kwanza basin, Angola: Marine and Petroleum Geology, v. 9, p. 405–411.

Nelson, T. H., 1989, Style of salt diapirs as a function of the stage of evolution and the nature of encasing sediment, *in* Gulf of Mexico salt tectonics, associated processes and exploration potential: SEPM Gulf Coast Section, 10th Annual Research Conference, Program and Extended Abstracts, Houston, Texas, p. 109–110.

Nelson, T. H., 1991, Salt tectonics and listric normal faulting, *in* A. Salvador, ed., The Gulf of Mexico basin: GSA Decade of North American Geology, v. J, p. 73–89.
Nilsen, K. T., 1994, Comments on the tectono-stratigraphic evolution of the Barents Sea (abs.): Tectonic and structural geology studies group meeting on reactivation of offshore and onshore basement structures: Norwegian Geological Society, Tromsø, Norway, Nov.
Nilsen, K. T., F. Henriksen, and G. B. Larssen, 1993, Exploration of the Late Paleozoic carbonates in the Southern Barents Sea—a seismic stratigraphic study, *in* T. Vorren, ed., Arctic geology and petroleum potential: Elsevier, Norwegian Petroleum Society, p. 393–403.
Nilsen, K. T., B. C. Vendeville, and J. T. Johansen, 1994, An example of salt tectonics controlled by regional tectonics: the Nordkapp Basin, Norway: AAPG Annual Convention Official Program, Denver, Colorado, v. 3, p. 225.
Nyland, B., L. N. Jensen, J. I. Skagen, O. Skarpnes, and T. Vorren, 1992, Tertiary uplift and erosion in the Barents Sea: magnitude, timing and consequences, *in* R. M. Larsen et al., eds., Structural and tectonic modelling and its application to petroleum geology: Norwegian Petroleum Society Special Publication, p. 153–162.
Reemst, P., S. Cloething, and S. Fanavoll, 1994, Tectono-stratigraphic modelling of Cenozoic uplift and erosion in the southwestern Barents Sea: Marine and Petroleum Geology, v. 11, p. 478–490.
Riis, F., 1992, Dating and measuring of erosion, uplift and subsidence in Norway and the Norwegian shelf in glacial periods, *in* L. N. Jensen et al., eds., Post-Cretaceous uplift and sedimentation along the western Fennoscandian shield: Norsk Geologisk Tidsskrift, v. 72, no. 3, p. 325–331.
Riis, F., and W. Fjeldskaar, 1992, On the magnitude of the late Tertiary and Quaternary erosion and its significance for the uplift of Scandinavia and the Barents Sea, *in* R. M. Larsen et al., eds., Structural and tectonic modelling and its application to petroleum geology: Norwegian Petroleum Society Special Publication, p. 163–185.
Riis, F., and L. N. Jensen, 1992, Measuring uplift and erosion—proposal for a terminology, *in* L. N. Jensen et al., eds., Post-Cretaceous uplift and sedimentation along the western Fennoscandian shield: Norsk Geologisk Tidsskrift, v. 72, no. 3, p. 320–324.
Rønnevik, H. C., 1982, Structural and stratigraphic evolution of the Barents Sea: Norwegian Petroleum Directorate Bulletin No. 1, 77 p.
Sales, J. K., 1992, Uplift and subsidence of northwestern Europe: possible causes and influence on hydrocarbon productivity: Norsk Geologisk Tidsskrift, v. 72, no. 3, p. 253–258.
Schultz-Ela, D. D., M. P. A. Jackson, and B. C. Vendeville, 1993, Mechanics of active salt diapirism: Tectonophysics, v. 228, p. 275–312.
Stemmerik, L., and D. Worsley, 1989, Late Paleozoic sequence correlations, North Greenland, Svalbard and the Barents shelf, *in* J. D. Collision, ed., Correlation in hydrocarbon exploration: Graham and Trotman, Norwegian Petroleum Society, p. 303–331.
Talbot, C. J., 1995, Molding of salt diapirs by stiff overburden, *in* M. P. A. Jackson, D. G. Roberts, and S. Snelson, eds., Salt tectonics: a global perspective: AAPG Memoir 65, this volume.
Talbot, C. J., H. Koyi, and J. Clark,1993, Multiphase halokinesis in the Nordkapp Basin, *in* T. O. Vorren et al., eds., Arctic geology and petroleum potential: Elsevier, Norwegian Petroleum Society, p. 665–668.
Vågnes, E., J. I. Faleide, S. T. Gudlaugson, 1992, Glacial erosion and tectonic uplift in the Barents Sea, *in* L. N. Jensen et al., eds., Post-Cretaceous uplift and sedimentation along the western Fennoscandian shield: Norsk Geologisk Tidsskrift, no. 3, p. 333–338.
Vendeville, B. C., 1993, Thin-skinned inversion tectonics of salt diapirs: GSA Abstracts with Programs, v. 25, no. 6, p. A408.
Vendeville, B. C., and M. P. A. Jackson, 1991, Deposition, extension, and the shape of downbuilding diapirs: AAPG Bulletin, v. 75, p. 687–688.
Vendeville, B. C., and M. P. A. Jackson, 1992a, The rise of diapirs during thin-skinned extension: Marine and Petroleum Geology, v. 9, p. 331–353.
Vendeville, B. C., and M. P. A. Jackson, 1992b, The fall of diapirs during thin-skinned extension: Marine and Petroleum Geology, v. 9, p. 354–371.
Vendeville, B. C., M. P. A. Jackson, and H. Ge, 1993a, Detached salt tectonics during basement-involved extension: AAPG Annual Convention, Official Program, New Orleans, Louisiana, p. 195.
Vendeville, B. C., M. P. A. Jackson, and R. Weijermars, 1993b, Rates of salt flow in passive diapirs and their source layers, *in* Rates of geologic processes: SEPM Gulf Coast Section, 10th Annual Research Conference, Program and Extended Abstracts, Houston, Texas, p. 269–276.
Vendeville, B. C., K. T. Nilsen, and J. T. Johansen, 1994, Using concepts derived from tectonic experiments to improve the structural interpretation of salt structures: the Nordkapp Basin example: Geological Society of London, meeting on modern developments in structural interpretation, validation and modelling, London, Feb. 21–23.
Vendeville, B. C., H. Ge, and M. P. A. Jackson, 1995, Models of salt tectonics during basement extension: Petroleum Geoscience, v. 1, p. 179–183.
Willoughby, J., and P. E. Øverli, 1994, Salt diapirism and the geological history of the western Nordkapp Basin: an exploration perspective (abs.): Tectonic and structural geology studies group meeting on reactivation of offshore and onshore basement structures, Norwegian Geological Society, Tromsø, Norway, Nov.
Yu, Z., and I. Lerche, 1993, Salt dynamics: simulation of mushroom cap on a salt diapir in the Barents Sea, Norway, *in* T. O. Vorren et al., eds., Arctic geology and petroleum potential: Elsevier, Norwegian Petroleum Society, p. 669–680.